
Article:
Zhang, S, Murray, BS orcid.org/0000-0002-6493-1547, Suriyachay, N et al. (3 more authors) (2021) Synergistic interactions of plant protein microgels and cellulose nanocrystals at the interface and their inhibition of gastric digestion of Pickering emulsions. Langmuir, 37 (2). pp. 827-840. ISSN 0743-7463

https://doi.org/10.1021/acs.langmuir.0c03148

Synergistic interactions of plant protein microgels and cellulose nanocrystals at the interface and their inhibition of gastric digestion of Pickering emulsions

Shuning Zhang[1], *Brent S. Murray*[1**], *Nuttaporn Suriyachay*[1], *Melvin Holmes*[1], *Rammile Ettelaie*[1], *Anwesha Sarkar*[1*]

[1] Food Colloids and Bioprocessing Group, School of Food Science and Nutrition, University of Leeds, Woodhouse Lane, Leeds LS2 9JT, UK

Corresponding Authors

*Email: A.Sarkar@leeds.ac.uk (Prof. A. Sarkar);

**Email: b.s.murray@leeds.ac.uk (Prof. B. S. Murray)

KEYWORDS

Pickering emulsion, pea protein microgel particle, cellulose nanocrystal, electrostatic attraction, particle-particle interface, Langmuir trough, *in vitro* gastric digestion

TOC

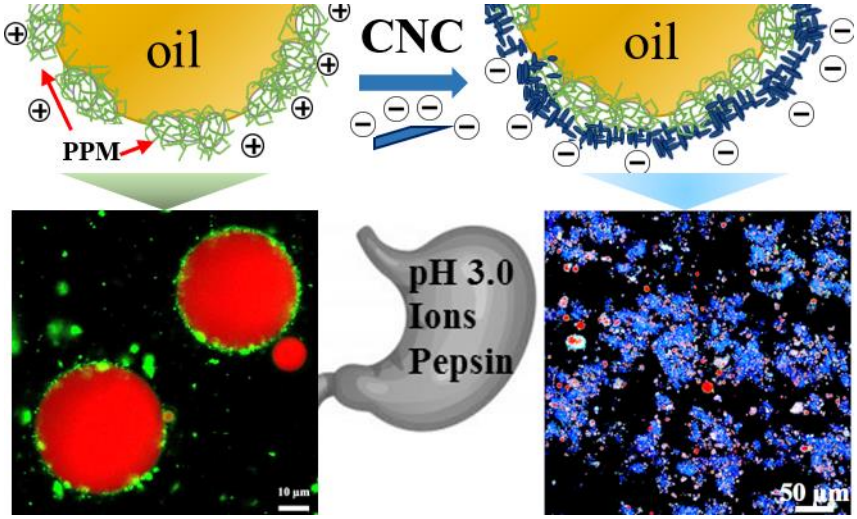

ABSTRACT

Pickering emulsions have possibilities for optimizing transport of nutraceuticals, pharmaceuticals and other bioactive compounds in human physiology. So-called ultra-stable Pickering emulsions can often get destabilized in the gastric digestion regime if the particles are proteinaceous in nature. The present study seeks to test how the interfacial structure can be engineered via synergistic particle-particle interactions to impact gastric coalescence of Pickering emulsions. In this study, we designed plant-based protein particle stabilized oil-in-water emulsions (PPM-E, with 20 wt% sunflower oil,) *via* pea protein microgels (PPM at 1 wt%). The PPM hydrodynamic diameter ≈ 250 nm. *In vitro* gastric digestion of PPM-E confirmed droplet coalescence within 30 min of pepsin addition. Supposedly surface active cellulose nanocrystals (CNCs, at 1-3 wt%) were added to PPM-E at pH 3.0, to see if could act as a barrier to interfacial pepsinolysis, due to the CNC and PPM being oppositely charged at this gastric pH value. A combination of confocal microscopy, zeta-potential and Langmuir trough measurements suggested that CNCs and PPMs might form a combined layer at the O/W interface, owing to the electrostatic attraction between them. CNCs at > 2 wt% inhibited pepsinolyis of the adsorbed PPM film and thus droplet coalescence. However, increasing concentrations of CNC also increased the bulk viscosity of the PPM-E and eventually caused gelation of the emulsions, which would also delay their gastric breakdown. In conclusion, tuning bulk and interfacial structure of

Pickering emulsions via synergistic interactions between two types of particles could be an effective strategy to modify enzymatic breakdown of such emulsions, which would have important applications in pharmaceuticals, foods and other soft matter applications.

INTRODUCTION

Pickering emulsions stabilized by biocompatible particles have aroused significant research interests recently owing to their extraordinary stability against coalescence due to their high desorption energies of the order of several thousands of k_BT (where k_B is Boltzmann constant and T is temperature) as opposed to < 5 k_BT for surfactant-stabilized emulsions and few hundreds of k_BT for biopolymer stabilized emulsions.[1, 2, 3, 4, 5, 6, 7, 8] Of more interest here is that emulsions stabilized by rigid solid particles via the Pickering stabilization mechanism or soft solid particles, which are often referred to as Mickering emulsions[7, 9] which have been used as novel vehicles to modulate lipid digestion in the human gastrointestinal (GI) tract to allow delivery of lipid soluble active compounds for pharmaceutical and food applications. This is largely attributed to the ability of these particles to be resistant against competitive displacement by surface active agents in human physiology such as bile salts.[10] In particular, proteinaceous particles from animal sources have shown abilities to retard lipid digestion in the intestines in the presence of pure lipase and bile salts, *i.e.*, bypassing gastric digestion by preventing displacement by bile salt, such as in the case of emulsions stabilized by whey protein microgel (WPM) particles with or without heat treatment[1] and lactoferrin nanoparticles (LFN).[2, 11, 12] In addition, non-proteinaceous particles such as chitin nanocrystals (CN),[13] have also shown abilities to retard lipid digestion by preventing displacement of particles by bile salt, as well as creating a network of chitin nanocrystals in the bulk phase, slowing down the transport of the enzyme to the oil-water (O-W) interface.

Although Pickering stabilization has shown promise in influencing digestion in the intestinal phase in a highly artificial environment - where a gastric phase has been by-passed, Pickering stabilizers

made from protein [12, 14, 15, 16] do not thrive in the preceding gastric regime, due to digestion by pepsin, and therefore will probably not offer any modulation of lipid digestion *in vivo*. For instance, protein particles, *e.g.* WPM,[1] LFN,[15] and karifin nanoparticles (KFN),[17] can be hydrolyzed by pepsin under the usual acidic gastric environments (pH 1.0 to pH 3.0), causing a rupture of the interfacial particulate film, leading to aggregation or coalescence of the droplets. Thus, a more protective interfacial architecture is required in the gastric phase in the case of Pickering emulsions stabilized solely by protein-based particles.

Regarding more complex interfaces, recent studies have shown success on improving the stability of O/W emulsions during *in vitro* gastric digestion via the formation of multilayers consisting of protein gel particles and polysaccharides. For instance, examples include the co-operative effects of LFN + carrageenan, alginate or pectin [11, 12, 15, 18], as well as between soy protein nanoparticles (SPN) and TEMPO-oxidized bacterial cellulose (TOBC) [16]. Layers coating the primary proteinaceous particle-stabilized interface, formed from polysaccharide-based particles such as cellulose nanocrystals (CNC), can act as an additional interfacial barrier, protecting the protein at the interface from being hydrolyzed by the gastric enzymes. This might be due to unique properties of CNC, in that is highly resistant to any human digestive enzymes and also the ability of CNCs to form particle networks in the continuous phase, which may slow down the transport of pepsin to the interface.[10]

In recent times, there has been a huge increase in the academic and commercial interest in exploiting and creating plant-based particles to design Pickering emulsions to replace animal-based proteins, due to their more 'vegan-friendly', 'environment-friendly', lower allergenicity and lower cost, *e.g.* zein particles,[19] kafirin particles,[17] soy protein nanoparticles (SPN).[20] For instance, Shao and Tang [21] created pea protein particles (PPP) at pH 3.0 and investigated the release of bioactive molecules from PPP-stabilized emulsions during lipid digestion. However, the required preparation of PPM at pH 3.0 limited the use of such emulsions during *gastrointestinal* lipid digestion. In the following study, a

new range of thermally-crosslinked pea protein microgels were created that can be used to stabilize O/W emulsions at a range of pH values: the stability of these emulsions was investigated here during *in vitro* gastric digestion. Furthermore, in order to provide the required improved stability for protein-stabilized systems[22], a more complex interfacial structure was created by adding in CNCs (unmodified). Since the CNCs used were manufactured via sulfuric acid treatment, this introduces some sulfate groups and therefore some negative charge and increased hydrophilicity [23, 24]. This results in the CNCs and PPMs having opposite charge at gastric pH values, so that they should form complexes at the interface and provide an additional barrier to the pepsin breaking down the primary PPM stabilizing film. Although several studies have shown mixed plant protein-polysaccharide particle interfaces can influence the rate of lipid digestion in a simulated digestion conditions [25], there have been relatively few reports of the effect of combining plant protein particle + unmodified CNC particles [16, 26]. A combination of sizing, zeta-potential measurements, microscopy across several length scales (confocal laser scanning microscopy and cryo-scanning electron microscopy (cryo-SEM), sodium dodecyl sulfate polyacrylamide gel electrophoresis analysis (SDS PAGE), bulk rheology and Langmuir trough experiments have been employed to understand the gastric fate and stability of O/W emulsions stabilized by both set of particles: PPM + CNC.

MATERIAL AND METHODS

Materials. Pea protein concentrate (Nutralys S85X) containing 85% protein was provided by Roquette (Lestrem, France). Cellulose nanocrystal powder (CNC), which contained 100% sulfated CNC was purchased from CelluforceTM (Quebec, Canada). Sunflower oil was purchased from the local supermarket (Tesco, UK). Pepsin (P7000) with measured enzymatic activity of 650 U/mg was purchased from Sigma-Aldrich (Dorset, UK). Mini-protein TGX gels, ProtoBlue safe colloidal Coomassie G-250 stain and all chemicals for sodium dodecyl sulfate polyacrylamide gel electrophoresis (SDS-PAGE) were purchased from Bio-Rad Laboratories, UK. All the chemicals, including sodium azide, Nile Red and Nile Blue, were of analytical grade and purchased from Sigma-

Aldrich (Dorset, UK) unless otherwise specified. All solutions used were prepared using Milli-Q water which was purified by a Milli-Q apparatus (Millipore Crop., Bedford, MA, USA) with an ionic purity of 18.2 MΩ·cm at 25℃.

Preparation of pea protein microgel particles (PPM). Pea protein microgel particles (PPM) were prepared using a process previously described by Zhang and coworkers.[27] Briefly, pea protein concentrate (12.54 wt% protein) was dispersed in 20 mM phosphate buffer at pH 7.0 for 2 h and then the protein dispersion was heated at 90 °C for 60 min to form pea protein hydrogels and cooled to room temperature followed by storage at 4 °C overnight. The hydrogels were then mixed with phosphate buffer (1:1 w/w) at pH 7.0 and then pre-homogenized using a kitchen blender (HB711M, Kenwood, UK) for 5 min at level 3. The aqueous dispersion of the macrogel particles was subsequently homogenized using two passes through a two stage valve homogenizer (Panda, GEA Niro Soavi Homogeneizador Parma, Italy) at a pressure of 250/ 50 bar. The resulting microscopic PPM dispersion contained 6.28 wt% protein. Sodium azide (0.02 wt%) was added to prevent microbial growth. The PPM dispersion was diluted with phosphate buffer to 1.25 or 3.33 wt% protein before the emulsion preparation.

Preparation of O/W emulsions

PPM-E emulsions at pH 7.0 were prepared by homogenizing 20.0 wt% sunflower oil with 80.0 wt% PPM the latter containing 1.25 wt% protein, at pH 7.0. The mixture of oil and aqueous phases was pre-homogenized using a Silverson rotor-stator type mixer (L5M-A, UK) at 8000 rpm for 5 min. The pre-emulsions were homogenized by two passes through the Panda homogenizer (GEA Niro Soavi Homogeneizador Parma, Italy) at 250/ 50 bar pressure. PPM-E + CNC emulsions were prepared as for PPM-E as above, but using 3.33 wt% protein in 60 wt% aqueous phase + 40 wt% oil, then adjusting the pH to pH 3.0 and mixing in a CNC dispersion (2-6 wt% in Milli-Q water at pH 3.0), waiting for 3 h, finally resulted in PPM-E + CNC emulsions containing 20 wt% oil, 1 wt% PPM

(*i.e.*,the same as PPM-E) + 1 to 3 wt% CNC. In the following we denote the CNC concentration in the PPM-E + CNC systems with a subscript, *e.g.*, PPM-E + $CNC_{1.0}$, for the system containing 1 wt% CNC.

In vitro gastric digestion. The PPM dispersion, PPM-E and PPM-E + CNC were digested using a digestion protocol designed by Minekus, et al. [28] Briefly, 10 mL of PPM dispersion (1 wt% protein) or emulsion sample (20 wt% oil, 1 wt% protein) at pH 3.0 was mixed with 10 mL of simulated gastric fluid (SGF), which contained 0.514 g L^{-1} KCl, 0.123 g L^{-1} KH_2PO_4, 0.042 g L^{-1} $NaHCO_3$, 0.06 g L^{-1} NaCl, 0.0004 g L^{-1} $MgCl_2(H_2O)_6$, 0.0009 g L^{-1} $(NH_4)_2CO_3$ and 2000 U mL^{-1} pepsin at pH 3.0 to simulate fed-state gastric digestion conditions. The mixture was incubated for 2.5 h at 37 °C using a shaking water bath (100 rpm, Grant Instruments Ltd, Cambridge, UK). To understand the changes in the physicochemical properties or structure of the microgel particles or droplets during the digestion, aliquots were collected at 0, 1, 5, 30, 60, 90, 120 and 150 min for size, zeta-potential, microscopy and SDS-PAGE analysis, and viscosity measurement. In the data collected during the digestion, "0 min" refers to the control sample, *i.e.*, the mixture of sample and SGF buffer without any added pepsin. For size and zeta-potential measurement, samples were measured immediately once collected from digested mixture. It is worth mentioning that the protocol's recommended oral phase was not used in this study, because the systems do not contain any starch and thus were not expected to have any pesinolysis digestion.

Measurement of PPM and emulsion droplet size. Particle sizes of aqueous dispersions of PPM as function of digestion time were determined via dynamic light scattering (DLS) at 25 °C using a Zetasizer Nano-ZS (Malvern Instruments, Malvern UK) in a standard PMMA disposable cuvette. The samples before and after gastric digestion were diluted 200 times in SGF buffer (pH 3.0). The hydrodynamic diameter (D_h) of the PPM was calculated using the Stokes–Einstein equation ($D_h = \frac{k_B T}{3\pi\eta D_t}$), where, D_t is the translational diffusion coefficient, k_B is Boltzmann's constant, T is temperature

in Kelvin, and η is dynamic viscosity of the aqueous dispersion of PPM. The refractive index of PPM was set at 1.52 with an absorbance of 0.001, as previously reported by Zhang, et al. [27]

Droplet size distributions of emulsions before and after digestion were determined via static light scattering (SLS) at 25 °C using Malvern MasterSizer 3000 (Malvern Instruments Ltd, Malvern, Worcestershire, UK). The samples were diluted to give an obscuration of between 4 and 6%. Refractive indices were set at 1.46 for sunflower oil and 1.33 for the aqueous medium, respectively. The average droplet size of the emulsion was reported as d_{43} (the volume mean diameter, $\frac{\sum n_i d_i^4}{\sum n_i d_i^3}$) and d_{32} (surface mean diameter, $\frac{\sum n_i d_i^3}{\sum n_i d_i^2}$) where, n_i is the number of droplets with a diameter, d_i.

Measurement of zeta-potential. Zeta-potentials of PPM dispersions, PPM-E and PPM-E + $CNC_{1\text{-}3}$ before and after digestion were measured using a Zetasizer Nano ZS (Malvern Instruments, Worcestershire, UK). Before adding into a folded capillary cell (DTS1070 cell, Malvern Instruments Ltd., Worcestershire, UK), samples were diluted to 0.01 wt% particle concentration or 0.008 wt% droplet concentration using SGF buffer at pH 3.0.

Microscopy. Cryogenic scanning electron microscopy (cryo-SEM) was used to visualize the adsorbed PPM and the arrangement of CNC at the interface of PPM-E or PPM-E + $CNC_{1\text{-}3}$, respectively. To avoid influence by oil crystallization during the freezing step, [3, 28, 29] heptane was used as the dispersed phase instead of sunflower oil. A droplet of the emulsion sample was filled into a copper holder before being flash frozen in liquid nitrogen at −180 °C. The samples were exposed to −95 °C for 5 min and then coated with 5 nm of platinum. Images were captured using a FEI Quanta 200 F ESEM with a Quorum Polar Prep 2000 cryo system at −135 °C.

To perform microstructural characterization of PPM-E and PPM-E + $CNC_{1\text{-}3}$ before and after digestion, confocal laser scanning micrographs (CLSM) were captured using a Zeiss LSM 700

confocal microscope (Carl Zeiss MicroImaging GmbH, Jena, Germany). Approximately, 5 mL of sample was mixed with100 μL of Nile Red (2% w/v in dimethyl sulfoxide), 500 μL of Fast Green (10% w/v in Milli-Q water) and 100 μL Calcofluor White to stain the oil, proteinaceous particles and CNC, respectively. Nile Red, Nile blue and Calcofluor White were excited at 514 nm, 633 nm and 410 nm, respectively. About 200 μL of xanthan gum (1 wt%) was added into the stained samples of the PPM-E and PPM-E + $CNC_{1\text{-}3}$ to reduce the Brownian motion of the oil droplets. The prepared samples were placed onto a microscope slide with cavity, covered with a cover slip and observed with a 63× (oil immersion) objective lens.

Rheology. The apparent viscosity (η_a) dynamic elastic modulus (G′) and dynamic loss modulus (G″) of the freshly prepared PPM-E and PPM-E + $CNC_{1\text{-}3}$ were determined at 25 °C using a Kinexus Ultra rheometer (Malvern Instruments Ltd, Malvern, UK). The apparent viscosities were recorded as a function of shear rates ranging from 0.1 to 1000 s^{-1}. Strain amplitude sweep tests were carried out with a shear strain range of 0.01-100% at 0.1 Hz frequency. Frequency sweep tests were then determined with an angular frequency range of 0.01-10 s^{-1} at a strain amplitude of 0.1% (i.e. in the linear viscoelastic regime). In order to characterize the flow type of the emulsions, the apparent viscosity curves were fitted using the Ostwald-de Waele model, $\eta_a(\dot{\gamma}) = K\dot{\gamma}^{n-1}$, where $\dot{\gamma}$ is the shear rate, *K* is the consistency index and *n* is the flow behaviour index.

Electrophoresis of proteins and their digestates. The protein and peptides compositions of the aqueous dispersions of PPM after hydrolysis by pepsin were determined via sodium dodecyl sulfate polyacrylamide gel electrophoresis (SDS-PAGE). Approximately, 50 μL of the PPM + SGF mixture after gastric digestion at different times (0, 1, 5, 10, 30, 60, 120 and 150 min) were mixed with 40 μL of SDS sample buffer (62.5 mM Tris-HCl, 2 wt% SDS, 25 wt% glycerol, 0.01 wt% bromophenol blue, pH 6.8) and 10 μL of dithiothreitol solution (DTT, 50 mM in final concentration), and heated at 95 °C for 5 min. Exactly, 5 μL of protein molecular weight (M_w) markers and 10 μL of each of the

samples were loaded into pre-cast Mini-PROTEAN 8–10% TGX Gels in a Mini-PROTEAN II electrophoretic unit (Bio-Rad Laboratories, Richmond, CA, USA). After running the gel at 200 V for about 30 min, the gel was placed in a fixing solution (a 50:40:10 vol% ratio of Milli-Q water: methanol: acetic acid) for 2 h, and stained for 2 h with Coomassie Blue solution, which consisted of 90% ProtoBlue Safe Colloidal Coomassie G-250 stain and 10% ethanol. The gels were imaged using a ChemiDoc™ XRS + System with image LabTM Software after de-staining overnight in Milli-Q water.

Langmuir trough monolayer experiments. Langmuir trough monolayer experiments were carried out to understand the interaction between PPM and CNC at the interface, as described in a recent work measuring particle-particle interactions at the air-water (A-W) interface [30]. Although these experiments were carried out at the A-W and not the oil-water (O-W) interface, they still should have revealed more information about the nature of the interactions at the surface of the emulsion droplets. The surface pressure was measured using a roughened mica Wilhelmy plate (3−5 cm in width), suspended from a force transducer (Maywood Instruments, Basingstoke, UK) at the center of a polytetrafluoroethylene (PTFE) trough. Buffer (pH 7.0 or pH 3.0) was added to the trough until the plate dipped into the A−W interface. The A-W interfacial area in the trough was reduced to the smallest possible and a vacuum line used to suck away the surface of the aqueous phase until the surface pressure π was < 0.1 m N m^{-1} and this remained < 0.1 m N m^{-1} on subsequent re-expansion (to the maximum trough area) and re-compression. For PPM experiments, a drop of an aqueous dispersion of PPM (0.46 wt% protein concentration) in a 100 µl syringe was slowly formed at the tip of the syringe and slowly lowered to touch the A-W interface, following by raising of the syringe tip. This was repeated until 100 µL of the PPM dispersion was spread. Suspensions of CNC alone (0.04 wt% CNC) were spread similarly. In all cases each 100 µl spreading process took 1 to 2 min and π versus area isotherms were measured 10 min after spreading. For experiments with PPM and CNC together, in one type of experiment 0.46 wt% PPM alone (at pH 3.0) was spread first, as above, then

after 10 min 100 µl of a 0.04 wt% CNC dispersion at pH 3.0 was spread at top of the PPM film. Mixed dispersions of PPM and CNC were also spread (see later). Spread films were compressed at a constant low speed[31, 32, 33] to measure the isotherms. In general, each spread film was compressed and expanded at least 2 times to check for reversibility, with all experiments conducted in triplicate.

Pepsin activity assay. In order to determine the effect of the presence of CNCs on pepsin activity, hemoglobin was used as reacting protein. [34] 500 µl hemoglobin dispersion (2% w/v) with or without 1-2 wt% CNC at pH 2.0 was incubated in a shaking water bath at 37℃ for 3 to 5 min to achieve temperature equilibration. Then 100 µL of pepsin solutions of different concentrations (5, 10, 15, 20, 25 and 30 µg/mL) were added into the hemoglobin or hemoglobin + CNC dispersions. After incubation for 10 min, 1 mL TCA (5% w/v trichloroacetic acid) was added to stop the activity of pepsin. Finally, the reacted solution was centrifuged at 6000 g for 30 mins to collect a clear solution for absorbance measurement, at 280 nm, known as the A_{280} Test. Hemoglobin or hemoglobin + CNC dispersions without pepsin were used as blanks. The pepsin activity is calculated *via* equation 1.

$$\text{Units/mg} = \frac{A_{280}\,Test \times 1000}{\Delta t \times X} \qquad \text{Equation 1}$$

Where, Δt is the duration of the reaction, *i.e.* 10 mins and X is the concentration of pepsin.

Statistical analyses. All measurements were done three times on triplicate samples prepared on separate days and were reported as the mean and standard deviation (n = 3 × 3). The statistical analyses were conducted using one-way (ANOVA) and the significant difference between samples were considered when $p < 0.05$ using Tukey test.

RESULTS AND DISCUSSION

Characteristics of aqueous dispersions of PPM. Pea protein microgel particles (PPM) dispersed in phosphate buffer at pH 7.0 were characterized to understand their properties before being used as Pickering emulsifiers. As shown in **Figure 1a**, DLS revealed a monomodal PSD (PSD) of PPM with

a single peak in the size range of 100-1000 nm, with a mean hydrodynamic diameter (d_h) of 250 nm and a low polydispersity index (PDI ~ 0.2), in line with previous reports.[27] The PPM at pH 7.0 had a negative charge with a measured ζ-potential (about -40 mV), since the pH of the PPM was above the isoelectric point (pI = 5.0).[27] The negatively-charged PPM suggests that the particles dispersed rather evenly in the aqueous solution without any visual separation due to the high particle-particle electrostatic repulsive forces.

In vitro *gastric digestion of aqueous dispersions of PPM.* It can be observed from **Figure 1b** that d_h of PPM + SGF mixture at pH 3.0 without pepsin has similar values to those of fresh prepared PPMs at pH 7.0 (~250 nm) (**Figure 1a**). Interestingly, PPM at pH 3.0 with SGF had a larger size value, *i.e.* 2-3 μm, where data by DLS should be interpreted cautiously.[27] **Figure 1b** shows that the zeta-potential of PPM at 0 min digestion was positive (+25 mV) due to the protonation of the ionizable groups at pH 3.0. This zeta-potential value was slightly lower than that measured previously in water,[27, 35] presumably due to the presence of the SGF ions.

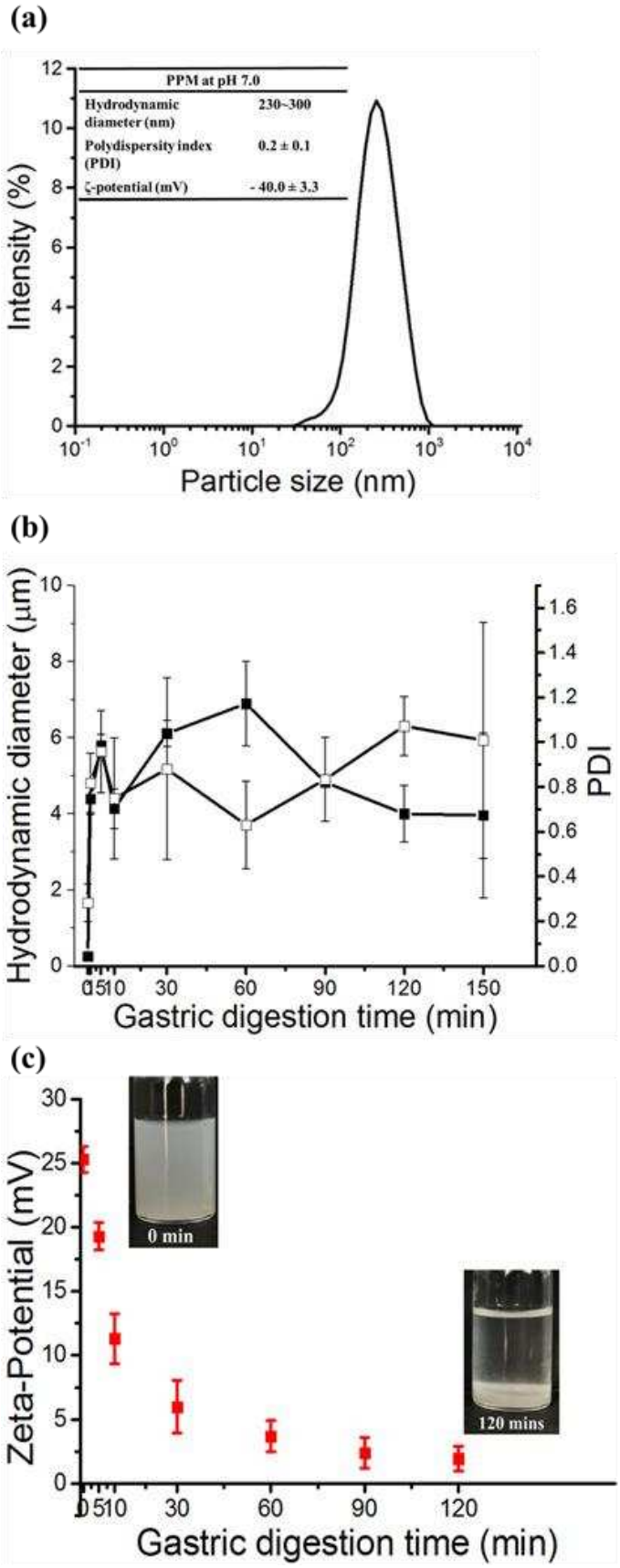

Figure 1. (a) PSD of pea protein microgel particles (PPM) at pH 7.0 with inset table showing the hydrodynamic diameter (d_h), polydispersity index (PDI) and zeta-potential. (b) and (c) Evolution of the mean d_H (■), PDI (□) and zeta-potential (■), respectively, of PPM at pH 3.0 after *in vitro* gastric digestion at different time points (0-120 min). The insets in (c) are images of aqueous dispersions of

PPM before and after 120 min of gastric digestion, respectively. Time 0 min represents the PPM + SGF mixture at pH 3.0 without the addition of pepsin. Error bars represent standard deviations.

In the presence of SGF containing pepsin, d_h of PPMs dramatically increased (from 0.25 to 7 μm, **Figure 1b**) within the first 60 min, comparing with the d_h of PPMs at 0 min ($p < 0.05$). This marked increase in the particle size of PPM with correspondingly high PDI values can be attributed to protein particle aggregation due to proteolysis, resulting in their eventual sedimentation, as evidenced by **Figure 1c**. Interestingly, d_h decreased slightly to 4 μm in the later stages of digestion (post 90 min), possibly due to the eventual breakdown of these aggregates by pepsin.[36] The zeta-potential of PPM rapidly reduced to ~5 mV within the first 30 min of digestion, and decreased to nearly zero at longer times (**Figure 1c**), partly explaining the increase in d_h because of a decrease in electrostatic repulsion between the particles.

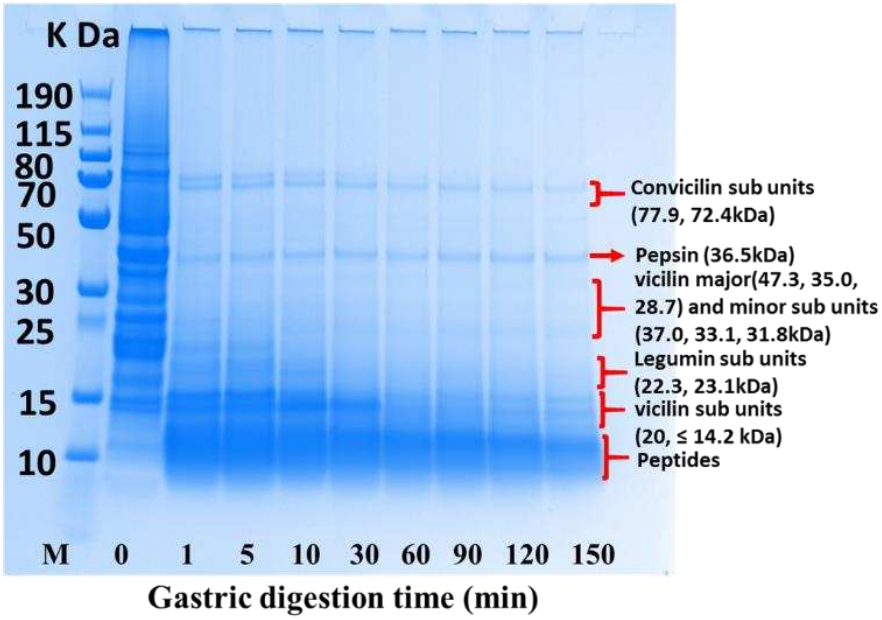

Figure 2. SDS-PAGE electrogram of aqueous dispersions of PPM at pH 3.0 after *in vitro* gastric digestion at different times (0-150 min). Lane M represents the protein markers of 10-250 kDa M_w range.

In order to better understand the gastric stability of PPM, the hydrolysis patterns of microgel particles containing 1 wt% protein were obtained using SDS-PAGE analysis, shown in **Figure 2**. In agreement

with the evolution in d_h and zeta-potential, PPM appeared to be digested immediately. All the major pea protein bands, especially convicilin (M_w = 77.9 kDa), legumin (M_w = 22.3, 23.1 kDa), vicilin (M_w = 47.3, 35.0, 28.7 kDa) and minor sub units (M_w = 37.0, 33.1, 31.8 kDa) disappeared within 30 min of digestion, except convicilin (M_w = 72.4 kDa) and vicilin subunits of Mw = 20 and $\leq$ 14.2 kDa). Both convicilin (M_w = 72.4 kDa) and vicilin sub units (M_w = 20 and $\leq$14.2 kDa) showed slow digestion and remained in significant proportions after 30 min and faint bands were visible even after 150 min digestion. According to the report by Laguna, et al. [22] post *in vitro* gastric digestion of pea protein isolate (PPI), only 20% of vicilin major sub units (M_w = 35.0 kDa) remained after 30 min in SGF containing pepsin, even with the much higher protein concentration used (*i.e*. 5 wt%). One might attribute the slower digestion in PPM compared to PPI due to the greater difficulty the enzyme has in penetrating into the microgel particles and accessing all the available substrate sites.[37] Opazo-Navarrete, et al. [38] compared pea protein concentrate and it's gels during gastric digestion and also demonstrated the ability of the gel structure to reduce enzyme diffusion. Similar results have been obtained when comparing whey protein, soy protein and egg white protein and their gel/microgel counterparts.[35, 38, 39]

PPM-stabilized Pickering emulsions (PPM-E). As shown in **Figure 3a**, the droplet size distribution of PPM-E at pH 7.0 was bimodal, consisting of a main peak in the size range 10 to 100 μm and a much smaller peak between 0.1 and 1 μm.

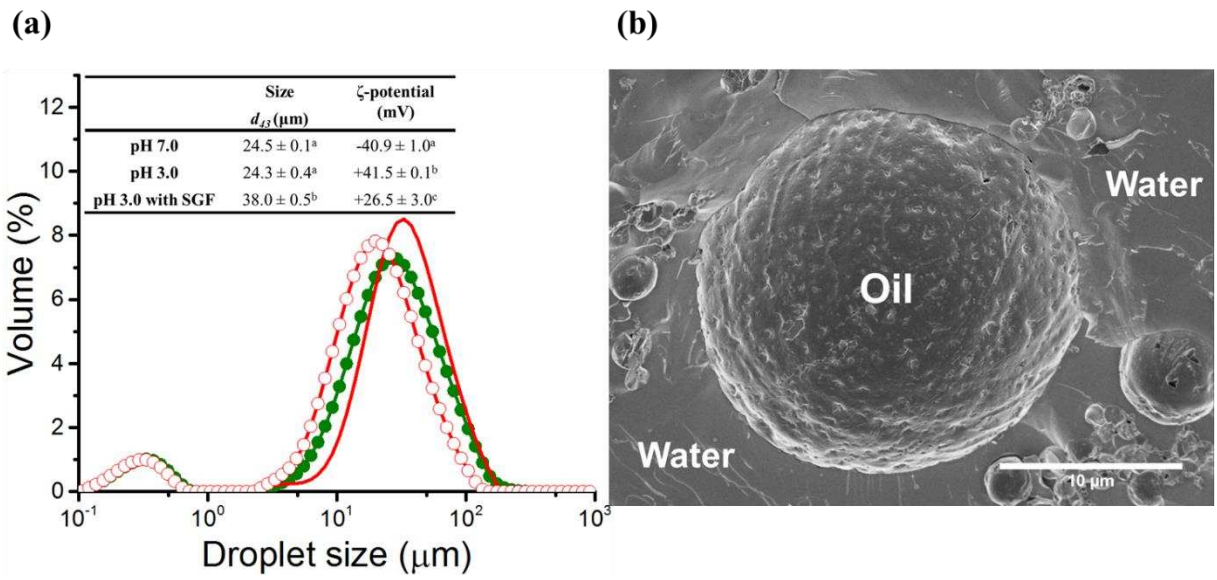

Figure 3. (a) Droplet size distribution of 20 wt% oil-in-water emulsions stabilized by PPM (PPM-E) at pH 7.0 (●), pH 3.0 (○) and PPM + SGF mixture at pH 3.0 without the addition of pepsin (-) with insets showing corresponding volume-average mean diameter (d_{43}) and zeta-potential of all the samples. Different superscripts (a-c) in the same columns of the inset of (a) represent significant differences between different samples at $p < 0.05$ level. (b) cryo-SEM micrograph of PPM-E at pH 7.0. Scale bar in (b) represents 10 μm.

Comparison with the microscopy of the emulsions suggests that the large peak represents the emulsion droplets whilst **Figure 1** suggests the small peak most likely corresponds to unabsorbed PPM, in line with previous studies.[27] Interestingly, there were no particles observed above 100 μm as seen with lactoferrin-stabilized emulsions under similar conditions, which was attributed to flocculation.[15] This suggests that sharing of PPM between droplets was not so obvious in this study and the amount of PPM was sufficient to cover the droplets.

The volume-average mean diameter (d_{43}) of PPM-E at pH 7.0 was around 25 μm and the zeta-potential was about –40 mV (**Figure 3a**), in agreement with previous work.[27] As such, the emulsions would be expected to exhibit long-term stability to coalescence. Efficient adsorption of the PPM particles to the oil-water (O/W) interface can be attributed to an increase in surface hydrophobicity of pea protein, resulting from the heat treatment[40] and agree with previous observations that 1% protein microgel particles of this sort of size can provide enough surface coverage to act as efficient Pickering stabilizers of 20 wt% O/W emulsions.[1, 3, 27] The cryo-SEM images (*e.g.*, **Figure 3b**) show

that the PPM appeared to cover the droplets effectively. In addition, there were no significant differences ($p > 0.05$) between the d_{43} of PPM-E at pH 7.0 and that at pH 3.0 (**Figure 3a**), even though the zeta-potential was reversed and so must have passed through zero on acidification. The reversal of the sign of the zeta-potential (from –40 mV to +42 mV) on acidification from pH 7.0 to pH 3.0 was expected from **Figure 1c** and because the isoelectric point of pea protein is between these two pH values.[27]

In vitro *gastric digestion of PPM-E.* As seen in **Figure 3a**, in the presence of SGF without pepsin, the mean droplet size of PPM-E (0 min) was comparable to that of the freshly prepared PPM-E at pH 3.0. However, the surface charge of PPM-E at 0 min incubation time (~27 mV) reduced slightly as compared to that before gastric digestion (~42 mV), presumably due to the presence of the SGF ions. As noted earlier for the PPM alone,[15] although the mean droplet size (d_{43}) increased ($p<0.05$), and the main peak in the size range 10 to 100 μm moved slightly to right (**Figure 3a**), this effect was not strong enough to influence the observed stability of the PPM-E, *i.e.*, the PPM-E should be stable under gastric conditions before pepsin starts to act.

With increasing incubation time the main peak (droplets) showed a narrowing and slight increase in height, whereas the smaller peak (unabsorbed PPMs) appeared to decrease in height and move to higher sizes (**Figure 4a**). It seems possible that this represents the pepsin preferentially hydrolyzing the PPM-based network between droplets as well as any unabsorbed PPMs, as opposed to the PPM adsorbed at the droplet surface. Interestingly, a similar droplet size distribution was found between PPM-E at 60 min and 90 min (**Figure 4a**) suggested that the digestion by pepsin was fairly complete within 1 h of gastric digestion time. In line with the droplet distribution behavior, mean droplet size (d_{43}) slightly decreased ($p < 0.05$) while the surface mean size (d_{32}) remained steady ($p > 0.05$) within the first 10 min of gastric digestion (**Figure 4b**).

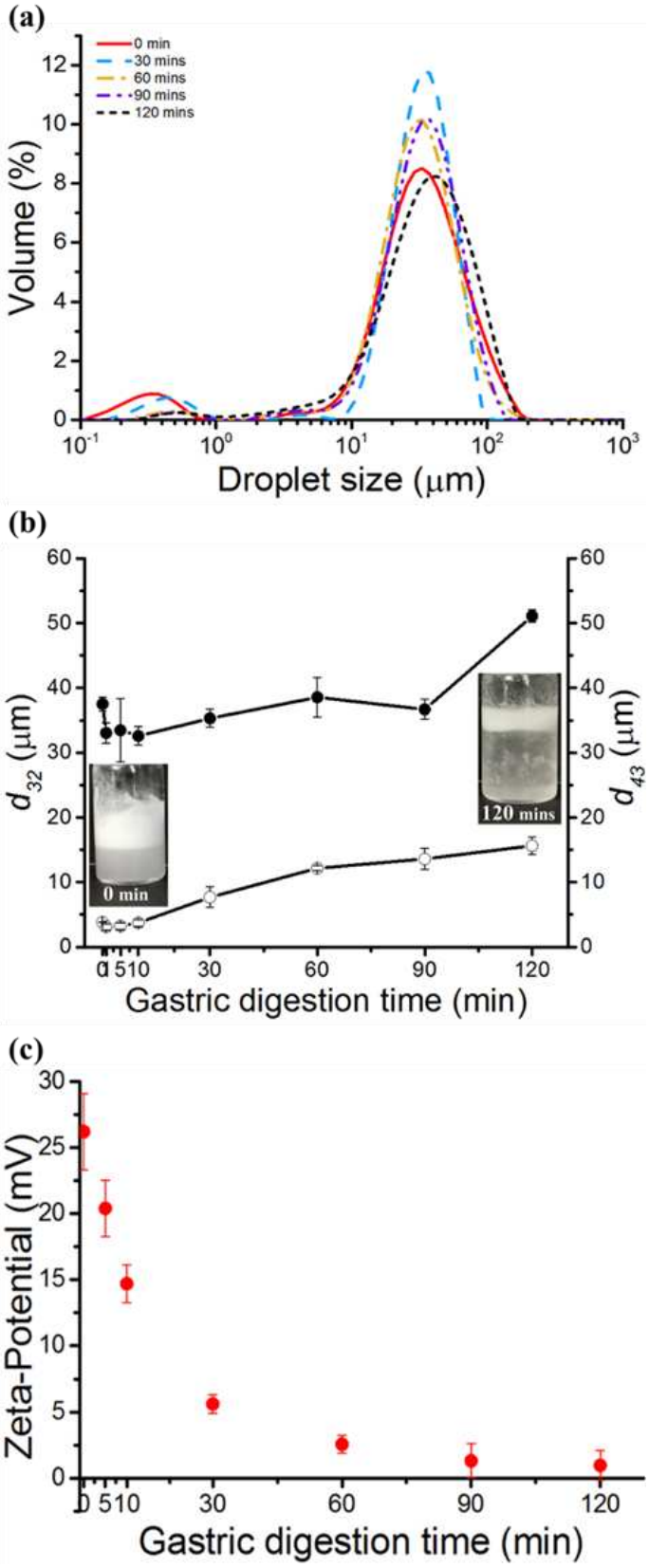

Figure 4. (a) Droplet size distribution, (b) d_{32} (○) and d_{43}, (●) and (c) zeta-potential (●), of PPM-E as a function of *in vitro* gastric digestion time with SGF containing pepsin. The insets in (b) are images of the emulsions before and after 120 min of gastric digestion. Time 0 min represents the PPM-E + SGF mixture at pH 3.0 without the addition of pepsin. Error bars represent standard deviations.

At 30 min, d_{43} slightly increased back to ~35 μm and d_{32} slightly rose to ~10 μm. Beyond this time the smaller peak (unabsorbed PPMs) tended to disappear completely whilst there was with a significant increase in both d_{43} and d_{32} (**Figure 4d**), suggesting the attack by pepsin led to droplet flocculation and/or coalescence [41, 42], as discussed later. It should be pointed out that there is no simple way of distinguishing the proportion or interfacial versus bulk microgels that are digested by the pepsin. Both populations are already relatively unfolded protein and therefore probably quite accessible to pepsin as a result of the method of their formation.

As can be seen in **Figure 4c**, the zeta-potential of the droplets was also dramatically reduced ($p < 0.05$) after 30 min incubation and was close to zero at the end of digestion time. This indicates, at least, that the composition of the PPM interfacial layer must change and/or the amount adsorbed is reduced, as might be expected from the SDS-PAGE hydrolysis pattern of PPM (**Figure 2**). As the PPM becomes hydrolyzed into smaller and smaller peptide chains these are expected to become less surface active and more water soluble, leading to less stable emulsions. **Figure 4b** clearly shows extensive creaming of the emulsions after 120 min digestion and there was evidence of some free oil floating on top of the gastric fluid.

The above results were clearly represented in the microstructural changes observed in the CLSM images (**Figure 5**). (Tiled images of the samples over larger areas are shown in **Supplementary Figure S1**.) With addition of pepsin, a clear sign of larger oil droplets was observed, confirming that droplets underwent coalescence within the first 30 min, in agreement with the changes in PSD, etc., seen in **Figure 4**. Similar CLSM observations have been made for a range of protein-based Pickering emulsions in gastric digestion conditions: whey protein microgels and 'nanoparticles',[1, 41] lactoferrin 'nanoparticles',[2, 15] and karifin 'nanoparticles'[17].

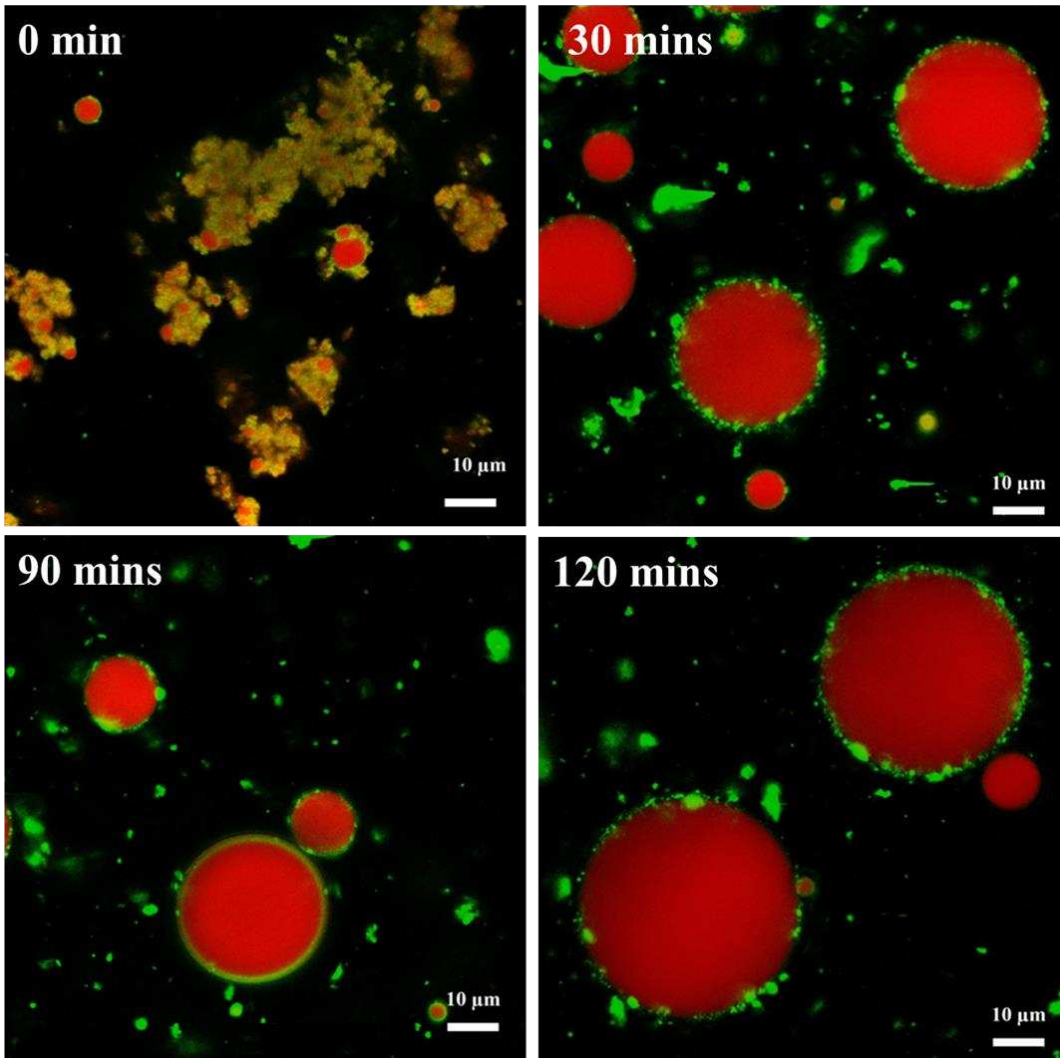

Figure 5. Confocal micrographs of 20 wt% oil-in-water emulsions stabilized by PPM (PPM-E) as a function of *in vitro* gastric digestion time (0-120 mins) at pH 3.0 (refer to **Supplementary Figure S1** for tiled confocal micrographs covering larger fields of view). Green color represents PPM (stained by Nile Blue); red color represents oil (stained by Nile Red); black color represents air or water. Time 0 min represents the PPM-E + SGF mixture at pH 3.0 without the addition of pepsin. Scale bar represents 10 µm.

Interactions between CNCs and PPM-E at pH 3.0. The CNCs used in this study were needle-like solid crystals with a diameter of ~100 nm. As reported in previous research,[10, 43, 44] and discussed in the introduction, the zeta-potential of CNC is relatively high (and negative) at pH 3.0. [23, 45, 46] Since the oil droplets in PPM-E had an opposite, positive zeta-potential (**Figure 3a**) at pH 3.0, adsorption of CNC onto the adsorbed PPM layer is expected with a change in the droplet zeta-potential to smaller +ve and even –ve values. As shown in **Figure 6a**, this is indeed the case - as the concentration of

CNC was increased from 0.5 to 4.0 wt%, the zeta-potential changed from +40 to –45 mV, mostly between 0.5 and 2.0 wt% CNC. (CNC added to PPM dispersions alone produced very much the same effect, as shown in **Supplementary Figure S2**). The slightly positively charged PPM-E + $CNC_{1.0}$ (+4 mV) suggests that the droplets were not completely coated with CNC at this lower CNC concentration (1 wt%). Beyond 2 wt% CNC the value of zeta-potential was almost stable, suggesting that at ≥ 2 wt% CNC the PPM-E droplets were 'completely' covered by CNC, so that excess CNC probably existed in the bulk phase at ≥ 2 wt% CNC. Note, however, the impossibility of complete coverage of a spherical surface, i.e., one with no gaps at all, with solid objects. Similar findings for the protein microgel-stabilized emulsions coated with polysaccharides have been reported elsewhere - where increasing the concentration of the polysaccharide led to full coverage and charge reversal of the droplets. [41, 42] Another important aspect is that at ≥ 2 wt%, the samples showed gel-like characteristics with limited visual flowability (see **Figure 6b**). Such behaviour was also seen in case of PPM alone with 3 wt% CNC added. This gel like behaviour has also been seen previously[44] in emulsions with hydrophically-modified CNCs added. So one must also be aware that these CNCs may effect the bulk rheology by forming CNC-CNC network or CNC-PPM network in the continuous phase and consequently may influence stability and digestibility of the emulsions. On the basis of the above results, CNC concentrations of 1, 2 and 3 wt% were selected for investigating the effect of CNCs on the gastric digestions of PPM-E, as described later.

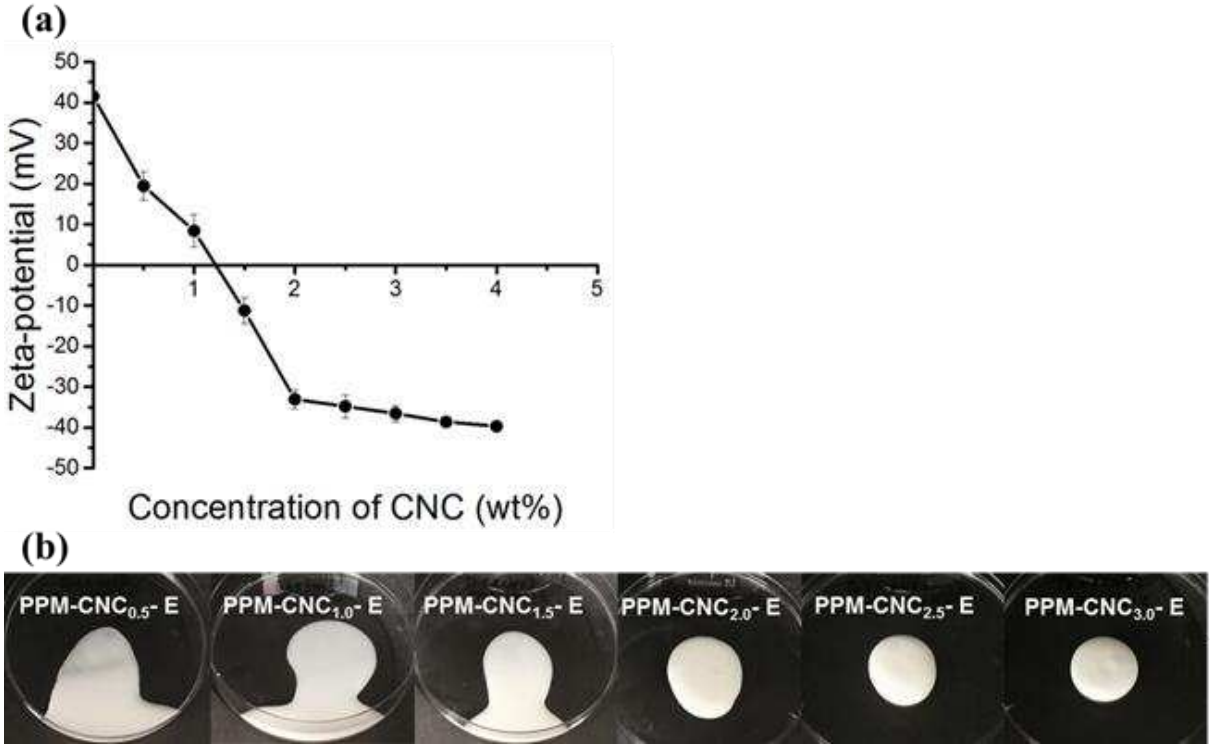

Figure 6. (a) Influence of concentration of cellulose nanocrystal (CNC) on zeta-potential (●); (b) corresponding visual images of PPM-E with added CNC. Error bars on (a) represent standard deviations.

Monolayer experiments on PPM and PPM + CNC. In order to further confirm the nature of the binding of CNC to PPM at the interface and to try and identify whether the PPM and CNC form multilayers or a single composite mixed film, surface pressure (π) versus area isotherms of PPM, CNC and PPM + CNC at air-water (A−W) interface were measured via the Langmuir trough-methods described above.

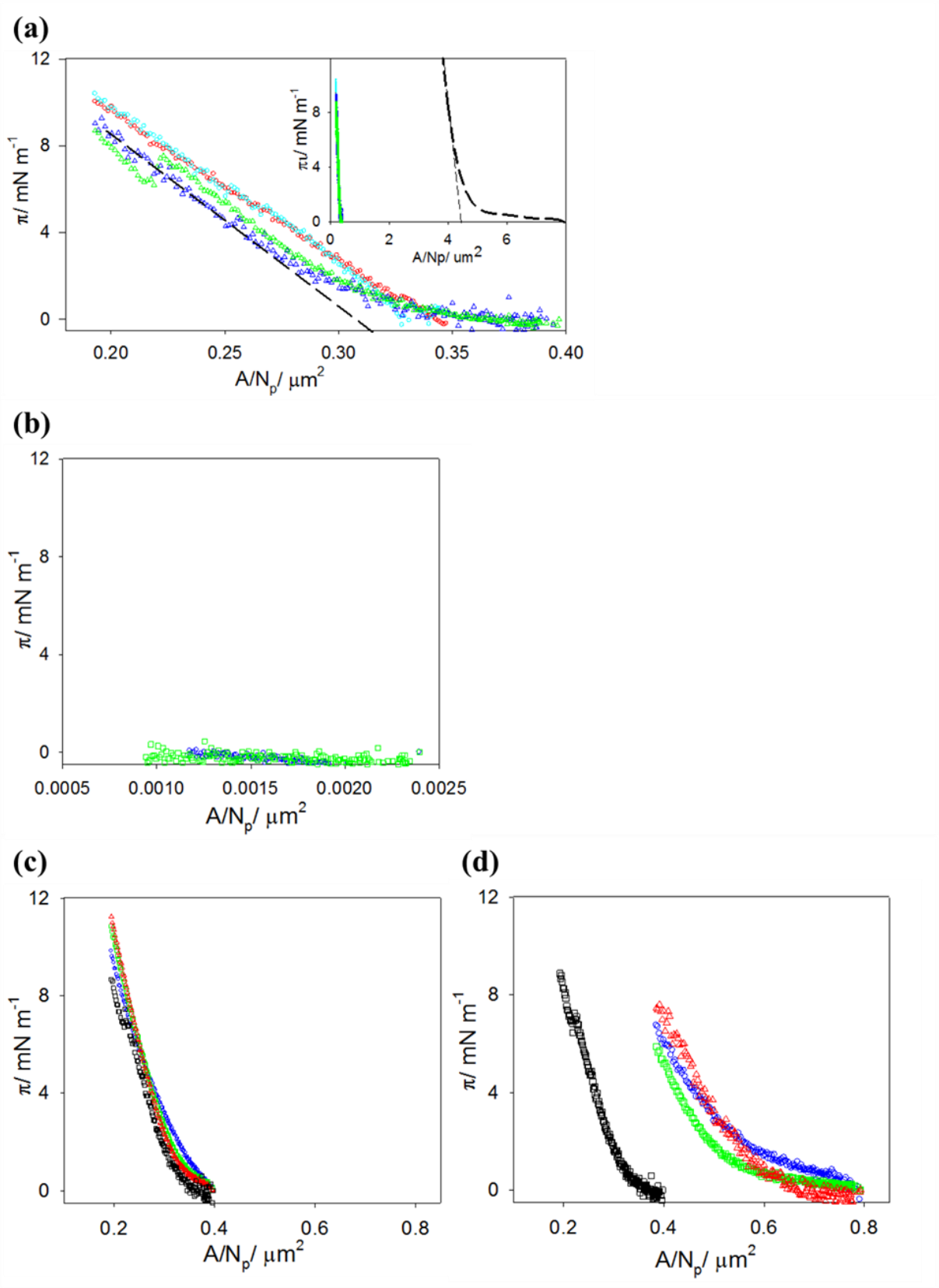

Figure 7. Surface pressure (π) versus area per particle (A/N_p) spread at the A-W interface for various systems. (a) 0.466 wt% PPM at pH 7.0 (○,○) and pH 3.0 (△,△): 1st compressions ○,△; 2nd compressions ○, △. (b) 0.04 wt% CNC alone at pH 3.0: 1st compression △; 2nd compression □. (c) 0.466 wt% PPM spread first at pH 3.0, followed by spreading of 0.04 wt% CNC on top of PPM: 1st compression ○; 2nd compression; □ 3rd compression △; average π-A/N_p result for 0.466 wt% PPM alone at pH 3.0 from (a) above □. (d) Mixture of 0.02 wt% CNC + 0.233 wt% PPM at pH 3.0: 1st

compression ○; 2nd compression; □ 3rd compression △; average π-A/N_p result for 0.466 wt% PPM alone at pH 3.0 from (a) above □. The dashed curve in the inset of Figure (a) shows the isotherm for whey protein microgels (WPM) taken from reference [30] compared to the pH 3.0 data for PPM in (a). The dashed straight lines in (a) are the extrapolations to estimate the dimensions of the adsorbed microgels (see text).

Figure 7a shows representative surface pressure (π) – area isotherms for 100 μL of 0.466 wt% PPM spread at the A-W interface at pH 3.0 and pH 7.0. A spherical PPM radius, r = 125 nm, according to the DLS data in **Figure 1a**, plus an assumed PPM particle density of 1 g cm^{-3}, were used to calculate the number of particles (N_p) spread from the mass of PPM spread. So the x-axis is the trough area (A) per particle, *i.e.*, A/N_p. In each case the film was compressed then expanded to the maximum trough area and compressed again, *i.e.*, compressed at least twice. For all PPM experiments, within experimental error, the repeated compression gave the same isotherm, confirming that the spread material was retained at the interface and/or any compression of the adsorbed microgel particles was reversible up to the π imposed on the film. It should be noted, however, that occasionally some small jumps in π were observed, which may indicate some film instability on compression (see below).

The isotherms for PPM at pH 7.0 appear to be displaced to slightly higher A/N_p than at pH 3.0, which might suggest greater expansion of the PPM at the pH 7.0 interface, due to their greater swelling and/or deformability at the higher pH value. Such effects would obviously be related to the different charges on the PPM at the two pH values. However, the **Supplementary Figure S3** shows the average values of π and their standard deviation for 3 separate experiments, compressed 3 times, *i.e.*, 9 isotherms for both pH 7.0 and pH 3.0 and it is seen that within experimental error there is negligible difference between the two, within the error of reproducibility. It is difficult make more accurate measurements because of the experimental difficulty of ensuring that none of the spreading solution is lost to the sub phase during the spreading, which is a common problem when spreading any proteinaceous material as opposed to completely insoluble surfactants. The inset to **Figure 7a** compares the average of the two isotherms for PPM at pH 3.0 in the main Figure with the average π v. A/N_p isotherm for whey protein microgels (WPM) also spread at pH 3.0, taken from previously

published work.[30] In this case the mean *r* of the WPM was 45 nm. The far more expanded isotherm for the WPM compared to the PPM is well within any experimental error, so that the PPM can be concluded to be far less deformed than WPM on adsorption at the A-W interface. For example, if the linear π-A/N_p region at the highest π is measured are extrapolated to the A/N_p axis, as shown by the straight dashed lines on **Figure 7a**, the intercept may be taken as the effective PPM cross-sectional area within the interface at which the PPM start to interact strongly. Assuming the PPM adopt a circular cross-sectional area of radius *r*′ and that the maximum 2-dimensional packing fraction[30] of these 'circles' is 0.9069, then the intercept of 0.31 μm^2 translates to *r*′ = 310 nm. It is seen that *r*′ is only moderately larger than *r* = 125 nm for the un-deformed PPM, whereas the equivalent *r*′ for WPM is ~ 4 x larger, despite *r* being smaller for WPM.[47, 48] Although instructive, such calculations ignore the wide distribution of microgel particle sizes (*e.g.*, see **Figure 1a**) and/or their aggregates and a lack of knowledge of the contact angles of such particle at the interface, so that absolute magnitude of these *r*′ values should be treated with caution. The main reason for the conducting the isotherm experiments was to gain more insight into the effect of CNCs when present in addition to PPM particles at the interface.

Figure 7b shows isotherms for 100 µl of 0.04 wt% CNC dispersion spread at the A-W interface at pH 3.0. CNC particle dimensions of a cylinder of diameter 6 nm and length 100 nm, plus a particle density of 1.5 g cm^{-3}, were used to calculate N_p spread. (The cylinder volume is equivalent to that of a sphere of radius only 8.8 nm, hence the much lower values of A/N_p, since N_p is so much higher despite the concentration spread being lower). It is seen that $\pi = 0 \pm 0.5$ mN m^{-1} for either the first or second compression. This experiment was repeated many times, sometimes increasing the CNC concentration spread, but the result was always the same. This suggests that the CNCs are not surface active enough to be retained by the A-W interface, but that they disperse into the aqueous subphase. **Figure 7c** shows isotherms for PPM spread as in **Figure 7a** at pH 3.0, but followed by spreading of 100 µl of 0.04 wt% CNC dispersion (as in **Figure 7b**) at the maximum trough area (*i.e.*, π = 0 mN m^{-}

[1]) on top of the PPM film. In view of the results in **Figure 7b**, it is perhaps not surprising that the PPM isotherm is not much affected by the addition of the apparently non-surface active CNC. Therefore, if any CNC particles that are associated with the adsorbed PPM they must be on top of (or below) the PPM layer and not within it.

Figure 7d shows the result of spreading 100 µl of a mixed solution of 0.0233 wt% PPM + 0.02 wt% CNC. Despite these PPM and CNC concentrations being half those in **Figures 7a-c**, the isotherm is much more expanded than that for the sequential addition in **Figure 7c**. In fact, this is why the concentrations had to be reduced in the spreading solution - to obtain a region where π tends to zero at the start of the compression. Thus, co-adsorbing PPM and CNC apparently leads to a much different film structure, presumably with some CNC embedded within the PPM film in the interfacial region – although we have no direct evidence for this as yet. However, this is not how the emulsion droplet interface is formed: PPM adsorbs first, stabilizing the emulsion and then CNC is added afterwards. Therefore, the adsorbed film structure is more likely to resemble that formed in the sequential adsorption experiment in **Figure 7c**, *i.e.*, if any CNC adsorbs it does so to the outside of the primary adsorbed PPM film. However, one should note that eventually the surface layers will approach the same final "equilibrium" composition and structure, irrespective of the sequence of addition of the particulate layers. Possibly the stark differences in the results illustrated in **Figures 7c and d** partly explain some of the apparent disagreements between the data in the literature concerning the surface activity (or not) of various CNCs. CNC may appear to be surface active when it is co-adsorbed with proteins but not on its own. Certainly the CNC used in these experiments has been shown elsewhere[44] not to depress the tension at the oil-water interface.

Particle size distributions of PPM-E with different CNC concentrations. As shown in **Figure 8a**, the PSDs of PPM-E + CNC with 1 to 3 wt% CNC at pH 3.0 were bimodal, with the largest peak between 1 and 100 µm. The smaller peak between 0.1 and 1 µm most likely represented free PPM

particles (as discussed earlier for the PPM-E emulsions) and/or free CNC particles and/or free PPM + CNC electrostatic complexes. The PSD in all of PPM-E + CNC systems was noticeably shifted to lower sizes compared to that of PPM-E at pH 3.0, in particular the main peak. This is consistent with significantly ($p < 0.05$) lower d_{43}: 16, 12 and 14 μm for 1, 2 and 3 wt% CNC respectively, suggesting that the CNCs reduce droplet flocculation. [15]

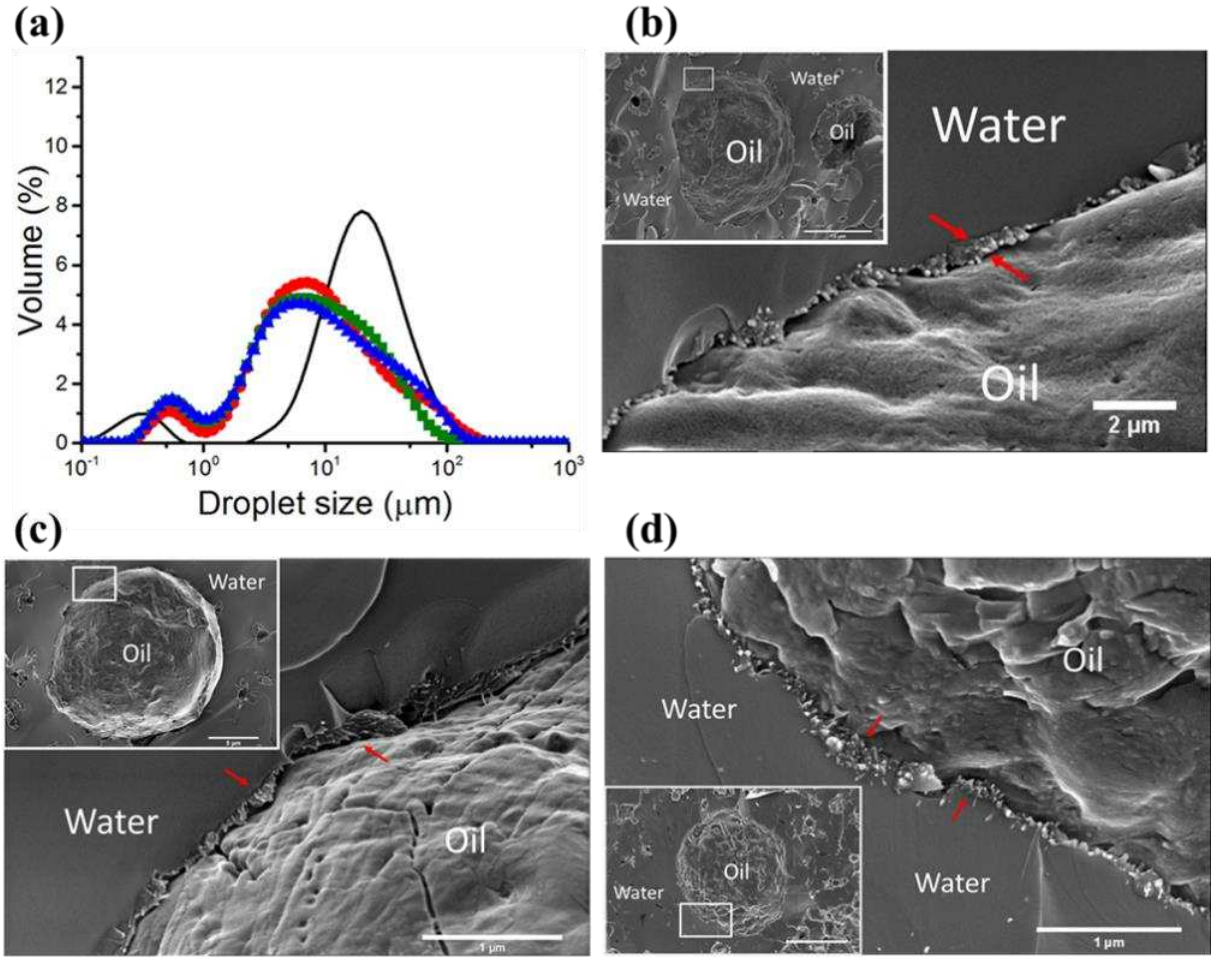

Figure 8. (a) PSDs of freshly prepared 20 wt% O/W emulsions at pH 3.0: stabilized by PPM only (PPM-E) (-); PPM-E with 1 wt% CNC (●), PPM-E with 2 wt% CNC (■); PPM-E with 3 wt% CNC (▲). Cryo-SEM micrograph and partial enlarged detail of PPM-E with: (b) 1 wt% CNC (c) 2 wt% CNC, (d) 3 wt% CNC (d). Scale bars represent in (b) 10 μm, in (c) and (d) 5 μm. The red arrows indicate what are thought to be CNC particles.

Interestingly, there was a slight increase of d_{43} when the CNC concentration was increased 2 wt% to 3 wt%, possibly due to depletion flocculation via excess CNC. [42] Cryo-SEM images in **Figure 8b-d** clearly show CNCs adsorbed on the surface of the PPM-stabilized emulsion droplets, which appeared

to have incomplete CNC surface coverage in case of PPM-E + $CNC_{1.0}$, and near full coverage in case of PPM-E + $CNC_{3.0}$.

Rheological properties of PPM-E + CNC emulsions. More detailed measurements were made on the influence of the CNCs on the viscoelasticity of the PPM-E + CNC emulsions (**Figure 9**). All emulsions with 1 to 3 wt% CNC were shear thinning over the shear rate ranging 0.1 to 1000 s^{-1} (**Figure 9a**), with the flow index (n) < 1 (**Table 1**). As the CNC concentration increased the consistency index (K) increased significantly ($p < 0.01$) (**Table 1**), suggesting a stronger attractive inter particle interaction between CNC-CNC and/or CNC-PPM. This was also supported by the optical images in **Figure 6b** based on the reduced flowability of PPM- E + CNCs at higher CNC concentration. At the same time, strain amplitude sweeps.

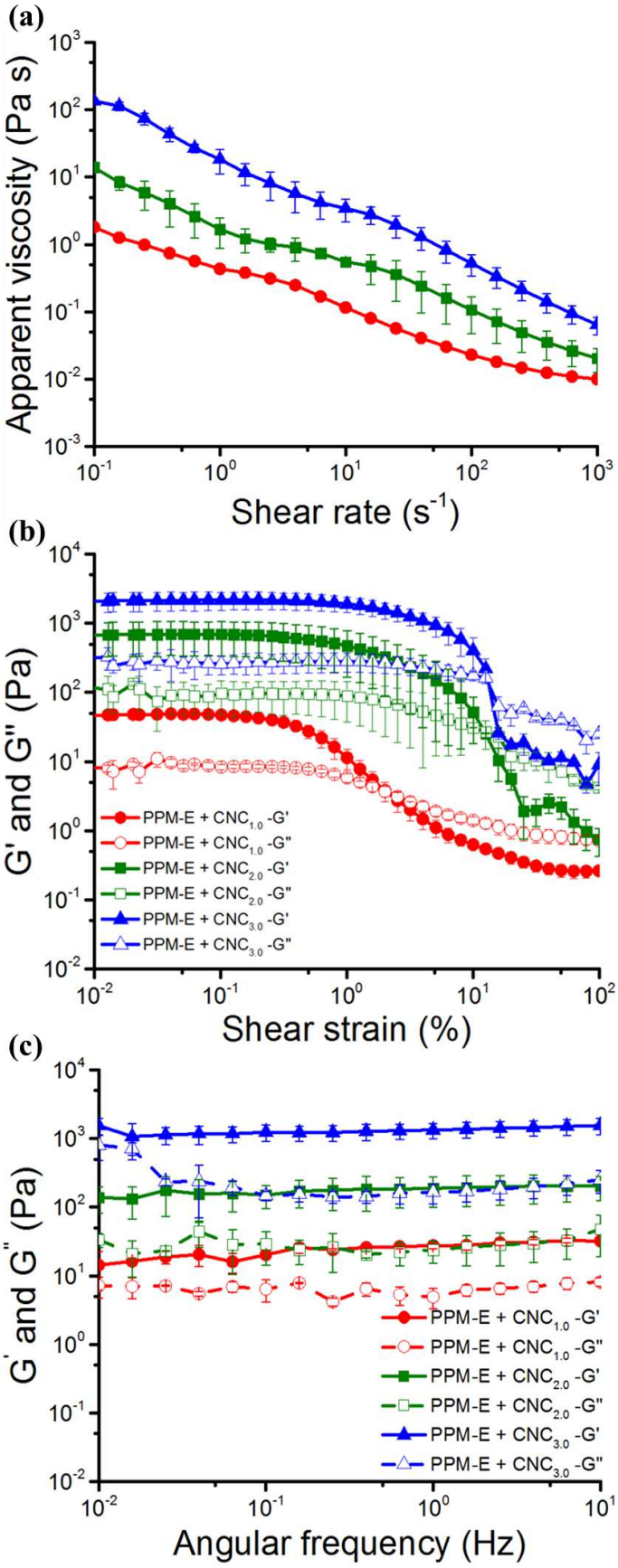

Figure 9. (a) Flow curves, (b) strain amplitude sweep curves, (c) frequency sweep curves of freshly prepared 20 wt% oil-in-water emulsions at pH 3 stabilized by PPM (PPM-E) with 1 wt% CNC (PPM-E + $CNC_{1.0}$) (●), 2 wt% CNC (PPM-E + $CNC_{2.0}$) (■) and 3 wt% CNC (PPM-E + $CNC_{3.0}$) (▲). Error bars represent standard deviations.

(**Figure 9b**) suggested that PPM-E with 2 wt% or 3 wt% CNC required a higher shear strain to break some sort of the network structure compared to 1 wt% CNC, as evidenced by the strain at which G′ and G′′suddenly started to decrease. **Figure 9c** shows the frequency sweep curves of G′ and G′′ versus with frequency (Hz) G′ > G′′ for all emulsions between 0.01 and 10 Hz, further suggesting a gel-like viscoelastic network in the presence of CNC,[16] particularly at the higher CNC concentrations.[49, 50, 51] Note that both G′ and G′′ for PPM-E + $CNC_{1.0}$ were higher than for PPM-E (**Figure 9c and Supplementary Figure S4**), *i.e.,* without CNC, confirming the essential nature of CNC to the network formation process.[49, 50] It is worth noting that both the shear thinning behaviour (**Supplementary Figure S5a**) and the gel-like behaviour (**Supplementary Figure S5b**) were also observed in PPM + CNC dispersions without oil, highlighting the influence of CNC in network formation in the bulk phase.

Table 1. Consistency index (*K*) and flow behaviour index (*n*) of PPM-E + 1, 2 or 3 wt% CNC.

Power-Law Model	***Ostwald de Waele fit for the apparent viscosity*** (η_a) $\eta_a(\dot{\gamma}) = K(\dot{\gamma})^{n-1}$		$\mathbf{R^2}$
	n	***K*** **(Pa s^n)**	
PPM-E + $CNC_{1.0}$	0.3 ± 0.1	0.5 ± 0.1[a]	0.95
PPM-E + $CNC_{2.0}$	0.3 ± 0.1	1.0 ± 0.3[b]	0.99
PPM-E + $CNC_{3.0}$	0.2 ± 0.1	18.1 ± 6.6[c]	0.93

Note: Different superscripts (a-c) in the same column represent significant differences between different samples at $p < 0.05$ level. The superscript *n* in units for *K* is the flow behavior index.

In vitro *gastric digestion of PPM-E + CNC*. As hypothesized, the presence of SGF without pepsin had only a slight effect on PPM-E + CNC (see **Figure 10**, **Supplementary Table S1** and **Table 2**). All the PPM-E + CNC emulsions at 0 min had no significant differences in the mean droplet size as compared to those of freshly prepared emulsions at pH 3.0. The zeta-potential of PPM-E + $CNC_{1.0}$ at 0 min was also the same as the freshly prepared emulsion ($p > 0.05$) (see **Supplementary Table S1** and **Table 2**), but the zeta-potential of both PPM-E + $CNC_{2.0}$ and PPM-E + $CNC_{3.0}$ at 0 min were

slightly less negative compared to the fresh emulsions. These results suggested that the droplets did not initially aggregate and so all the PPM-E + CNC were stable in the absence of pepsin action, similar to the behaviour of the PPM-E noted earlier.

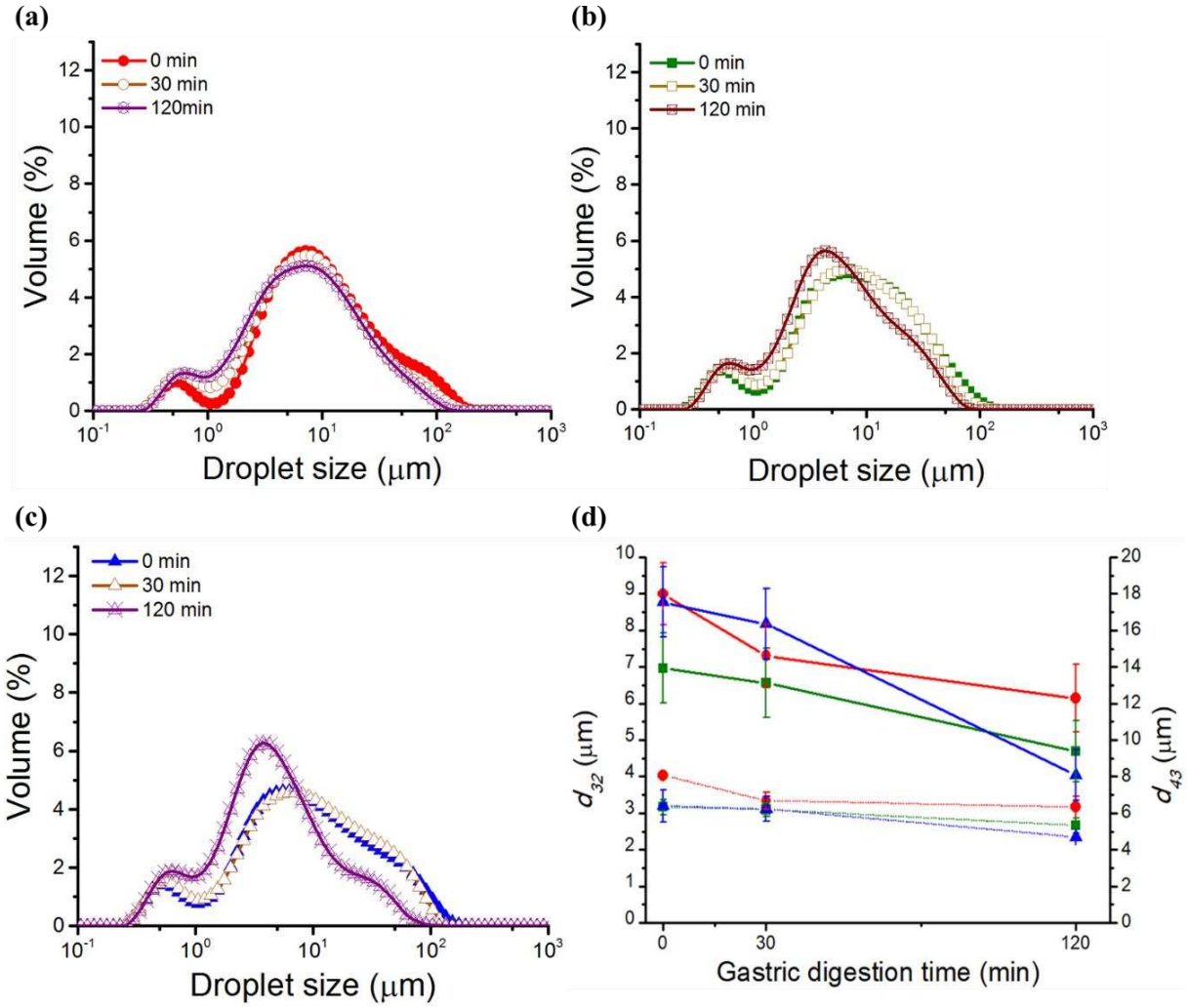

Figure 10. PSDs of PPM-E with: (a) 1 wt%, (b) 2 wt%, (c) 3 wt% CNC after different *in vitro* gastric digestion times. Time 0 min represents the emulsion + SGF mixture at pH 3.0 without the addition of pepsin. (d) Shows d_{32} (⋯) and d_{43} (-) at 0, 30 and 120 min for 1 (●), 2 (■) and 3 wt% CNC (▲). Error bars represent standard deviations.

Table 2. Mean zeta-potential of PPM-E with 1, 2 and 3 wt% CNC after 0, 30 and 120 min *in vitro* gastric digestion. Time 0 min represents the emulsion + SGF mixture at pH 3.0 without the addition of pepsin. Different superscripts (a-b) in the same column indicate significant differences between different samples at $p < 0.05$ level.

Mean zeta-potential (mV)	**Digestion time (min)**		
	0	**30**	**120**
PPM-E + $CNC_{1.0}$	5.9 ± 1.3^{a}	-5.5 ± 2.5^{b}	-8.8 ± 1.4^{b}
PPM-E + $CNC_{2.0}$	-29.7 ± 3.2^{a}	-18.5 ± 1.5^{b}	-20.5 ± 2.7^{b}
PPM-E + $CNC_{3.0}$	-34.3 ± 2.5^{a}	-26.1 ± 2.5^{b}	-26.0 ± 2.5^{b}

After being incubated in SGF with pepsin, the mean droplet size (d_{43}) of PPM-E + $CNC_{1.0}$ showed no significant change during gastric digestion for 2 h (**Figure 10d** and **Supplementary Table S1**) whilst there was an increase in the vol% of the minor peak between 0.1 and 1 μm in the first 30 min (**Figure 10a**) and a significant decrease in the d_{32}, as summarised in **Figure 10d** and **Supplementary Table S1**. This suggests the pepsin digested the aggregated network of unabsorbed PPM particles in the first 30 min, freeing up more primary emulsion droplets. Both PPM-E + $CNC_{2.0}$ and PPM-E + $CNC_{3.0}$ showed similar changes: d_{32} and d_{43} remained constant ($p > 0.05$) within the first 30 min (**Figure 10d** and **Supplementary Table S1**), whilst there was a similar increase in the vol% of the minor peak (**Figure 10b, c**) but the mean particle sizes had decreased considerably ($p < 0.05$) after 120 min digestion (**Figure 10d** and **Supplementary Table S1**). A possible explanation for these reduced mean particle sizes might be that pepsinolysis of the aggregated network of PPM. It was also thought the CNCs might reduce pepsin activity by either binding or trapping the enzyme in the CNC network in the continuous phase. This was confirmed via the pepsin activity assay with 2% w/v protein (haemoglobin) mixed with CNC, as showed in **Table 3**. The pepsin activity reduced from ~655 U/mg to 100-160 U/mg after adding CNCs to the protein dispersion. Consequently, the CNC can reduce pepsinolysis and breakdown of the PPM-stabilized emulsions in two ways: (i) binding to the PPM-laden interface and (ii) bonding or trapping the enzyme.

Table 3. Pepsin activity assay with 2 % w/v hemoglobin mixed with 1 wt% or 2 wt% CNC.

Substrate	Pepsin activity (U/mg)
Haemoglobin	654.7 ± 53.4^{a}
Haemoglobin+ $CNC_{1.0}$	133.8 ± 109.3^{b}
Haemoglobin + $CNC_{2.0}$	158.8 ± 97.8^{b}

Note: Different superscripts (a-b) in the same column represent results with significant differences between different samples at $p < 0.05$ level.

PPM-E + $CNC_{1.0}$ droplets showed a significant change in zeta-potential ($p < 0.05$) after simulated

gastric digestion (see **Table 2**). The zeta-potential changed from ~ +6 mV to −6 mV within 30 min, followed by a more gradual change to −9 mV by the end of the digestion time. This seems to indicate a loss of PPM from the interface. However, there was no increase in mean droplet size, as mentioned before. Since a negative value of zeta would seem to indicate the predominance of CNC at the interface, the peptide fragments produced by hydrolysis combined with the CNC must form a new type of protective shell surrounding oil droplets, preventing coalescence. Both PPM-E + $CNC_{2.0}$ and PPM-E + $CNC_{3.0}$ showed a significant change in zeta-potential ($p < 0.05$) after 30 min, zeta-potential changing from −30 mV to −20 mV and from −35 mV to −26 mV, respectively. In the case of PPM-E + $CNC_{3.0}$, this was followed by a stable zeta-potential until the end of the digestion time.

Confocal micrographs of PPM-E + CNC emulsions before and after digestion, shown in **Figure 11**, also provide evidence that no large coalesced oil droplets were formed after 2 h incubation, except PPM-E + $CNC_{1.0.}$ Interestingly, the blue color, *i.e.*, the stain for cellulose in the micrographs before digestion with increasing CNC concentration is enhanced, *i.e.*, darker blue, suggesting concentration of the CNC into specific regions. These regions probably represent the gel-like network in bulk that get stronger with increasing CNC concentration, as discussed above. The inset to the micrographs are photographs of the emulsions and show that no phase separation was observed, emphasizing again the greater stability of the emulsions to gastric digestion when CNC was added.

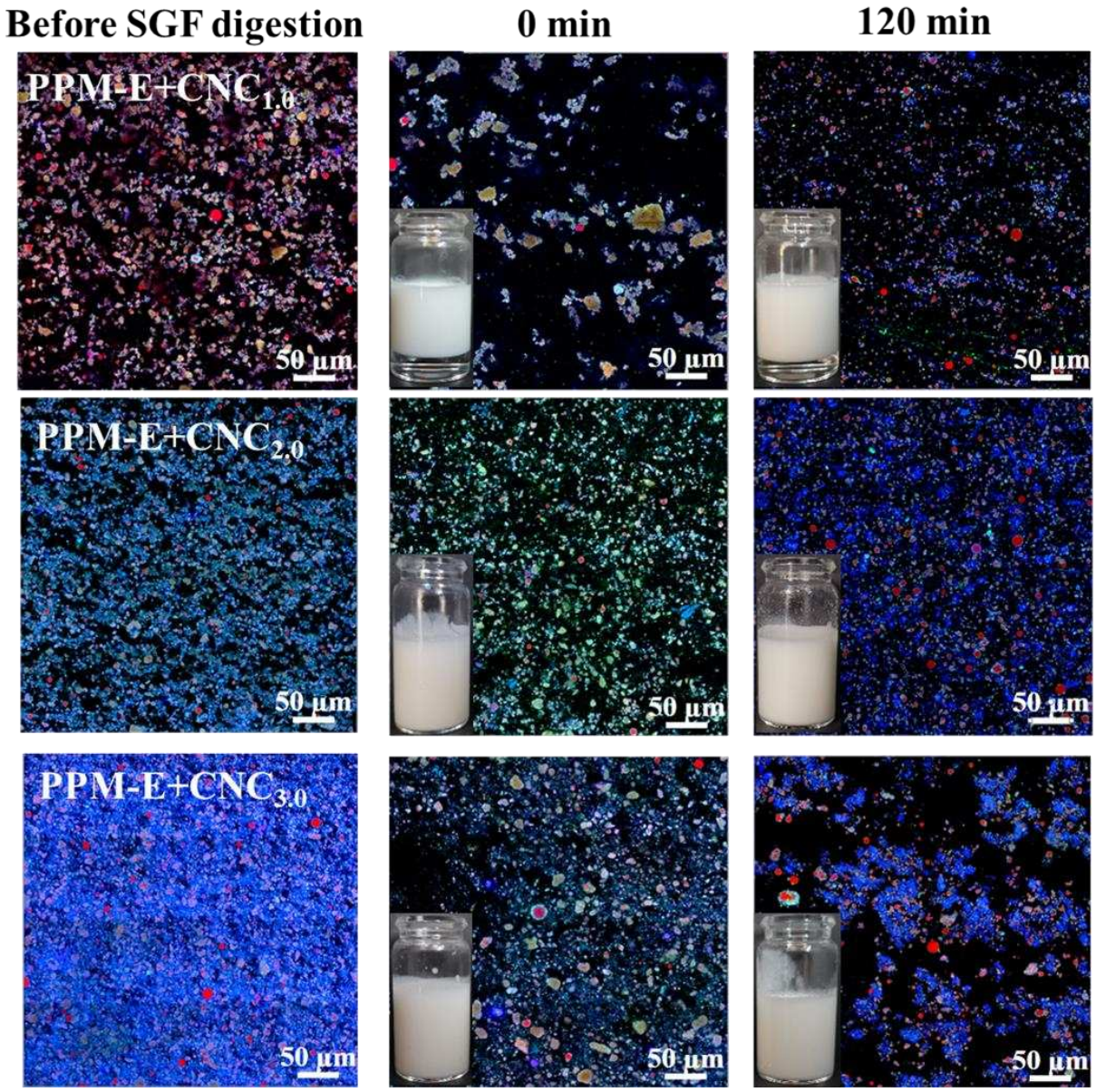

Figure 11. Confocal micrographs of 20 wt% oil-in-water emulsions stabilized by PPM (PPM-E) and 1 wt% CNC (PPM-E + $CNC_{1.0}$), 2 wt% CNC (PPM-E + $CNC_{2.0}$), and 3 wt% CNC (PPM-E + $CNC_{3.0}$) as a function of *in vitro* gastric digestion time (0, 120 min) at pH 3.0. The green color represents PPM (stained by Nile Blue); the red color represents the oil phase (stained by Nile Red); the blue color represents the CNC (stained by Calcofluor White); the black color represents air or water. Time 0 min represents the PPM-E + SGF mixture at pH 3.0 without the addition of pepsin. Scale bar represents 50 µm.

CONCLUSIONS

This study set out to understand the *in vitro* gastric digestion fate of Pickering O/W emulsions stabilized by pea protein microgels (PPM) with and without added cellulose nanocrystals (CNC). The study confirms that emulsion droplets stabilized by pea protein microgels alone break down completely when subjected to *in vitro* gastric digestion conditions, which causes droplet coalescence and phase separation. Addition of CNC stabilizes the emulsions against these effects. The added stability may be the result of the CNCs binding electrostatically to the outside of the adsorbed PPM layer at low pH, for which there is good evidence from zeta-potential and Langmuir trough experiments. On the other hand, rheological measurements indicate that the CNCs also induce the formation of a strong gel-like structure in the emulsions and it has also been shown that this CNC network can bind or trap the pepsin enzyme responsible for the digestion. This CNC-induced gelation and/or binding of the enzyme to the CNCs may restrict the access of the pepsin to the substrate sites available in the PPM and so contribute to the greater gastric stability of the emulsions. Such emulsions, based on complex plant-based particulate interfaces might be used to deliver bioactive molecules that require protection in the gastric regime. Future studies are focusing on how composite particulate layers can offer modulation of intestinal digestion of droplets.

ASSOCIATED CONTENT

Supporting information.

This material includes the confocal micrograph tiles covering different fields within the sample of emulsions stabilized by PPM (PPM-E) before and after *in vitro* gastric digestion (Figure S1), influence of concentration of cellulose nanocrystals (CNC) on mean ζ-potential values of aqueous dispersion of PPM and images of flowability of these mixtures (Figure S2), surface pressure versus area per particle spread at the A-W interface for PPM (Figure S3), frequency sweep curves of freshly prepared emulsions stabilized by PPM (PPM-E) at pH 3.0 (Figure S4), flow curves and frequency sweep curves of freshly prepared PPM (1 wt%) at pH 3 mixed with 1-3 wt% CNC (Figure S5) and mean droplet size of PPM-E with 1-3 wt% CNC after *in vitro* gastric digestion (Table S1).

AUTHOR INFORMATION

Corresponding Authors

*Email: A.Sarkar@leeds.ac.uk (Prof. A. Sarkar);

**Email: b.s.murray@leeds.ac.uk (Prof. B. S. Murray)

Food Colloids and Bioprocessing Group, School of Food Science and Nutrition, University of Leeds, Woodhouse Lane, Leeds, LS2 9JT, United Kingdom.

NOTES

The authors declare no competing financial interests.

REFERENCES

1. Sarkar, A.; Murray, B.; Holmes, M.; Ettelaie, R.; Abdalla, A.; Yang, X. In vitro digestion of Pickering emulsions stabilized by soft whey protein microgel particles: influence of thermal treatment. *Soft Matter* **2016,** *12* (15), 3558-69.
2. Shimoni, G.; Shani Levi, C.; Levi Tal, S.; Lesmes, U. Emulsions stabilization by lactoferrin nano-particles under in vitro digestion conditions. *Food Hydrocolloids* **2013,** *33* (2), 264-272.
3. Araiza-Calahorra, A.; Sarkar, A. Pickering emulsion stabilized by protein nanogel particles for delivery of curcumin: Effects of pH and ionic strength on curcumin retention. *Food Structure* **2019,** *21*, 100113.
4. Dickinson, E. Use of nanoparticles and microparticles in the formation and stabilization of food emulsions. *Trends in Food Science & Technology* **2012,** *24* (1), 4-12.
5. Dickinson, E. Microgels — An alternative colloidal ingredient for stabilization of food emulsions. *Trends in Food Science & Technology* **2015,** *43* (2), 178-188.
6. Sarkar, A.; Dickinson, E. Sustainable food-grade Pickering emulsions stabilized by plant-based particles. *Current Opinion in Colloid & Interface Science* **2020,** *49*, 69-81.
7. Murray, B. S. Pickering emulsions for food and drinks. *Current Opinion in Food Science* **2019,** *27*, 57-63.
8. Murray, B. S. Microgels at fluid-fluid interfaces for food and drinks. *Advances in Colloid and Interface Science* **2019,** *271*, 101990.
9. Gong, Y.; Wang, M.; He, J. The behavior of hydrophobic-core/hydrophilic-shell structured microgels at an interface: from Mickering emulsion to colloidosomes with dual-level controlled permeability. *RSC Advances* **2016,** *6* (97), 95067-95072.
10. Sarkar, A.; Zhang, S.; Holmes, M.; Ettelaie, R. Colloidal aspects of digestion of Pickering emulsions: Experiments and theoretical models of lipid digestion kinetics. *Adv Colloid Interface Sci* **2019,** *263*, 195-211.
11. Meshulam, D.; Lesmes, U. Responsiveness of emulsions stabilized by lactoferrin nano-particles to simulated intestinal conditions. *Food & function* **2014,** *5* (1), 65-73.
12. Peinado, I.; Lesmes, U.; Andres, A.; McClements, J. D. Fabrication and morphological characterization of biopolymer particles formed by electrostatic complexation of heat treated lactoferrin and anionic polysaccharides. *Langmuir* **2010,** *26* (12), 9827-34.
13. Tzoumaki, M. V.; Moschakis, T.; Scholten, E.; Biliaderis, C. G. In vitro lipid digestion of chitin nanocrystal stabilized o/w emulsions. *Food Funct* **2013,** *4* (1), 121-9.
14. French, D. J.; Brown, A. T.; Schofield, A. B.; Fowler, J.; Taylor, P.; Clegg, P. S. The secret life of Pickering emulsions: particle exchange revealed using two colours of particle. *Sci Rep* **2016,** *6*, 31401.
15. Sarkar, A.; Ademuyiwa, V.; Stubley, S.; Esa, N. H.; Goycoolea, F. M.; Qin, X.; Gonzalez, F.; Olvera, C. Pickering emulsions co-stabilized by composite protein/ polysaccharide particle-particle interfaces: Impact on in vitro gastric stability. *Food Hydrocolloids* **2018,** *84*, 282-291.
16. Zhang, X.; Liu, Y.; Wang, Y.; Luo, X.; Li, Y.; Li, B.; Wang, J.; Liu, S. Surface modification of cellulose nanofibrils with protein nanoparticles for enhancing the

stabilization of O/W pickering emulsions. *Food Hydrocolloids* **2019,** *97*, 105180.
17. Xiao, J.; Li, C.; Huang, Q. Kafirin nanoparticle-stabilized Pickering emulsions as oral delivery vehicles: Physicochemical stability and *in vitro* digestion profile. *J Agric Food Chem* **2015,** *63* (47), 10263-70.
18. David-Birman, T.; Mackie, A.; Lesmes, U. Impact of dietary fibers on the properties and proteolytic digestibility of lactoferrin nano-particles. *Food Hydrocolloids* **2013,** *31* (1), 33-41.
19. Filippidi, E.; Patel, A. R.; Bouwens, E. C. M.; Voudouris, P.; Velikov, K. P. All-natural oil-filled microcapsules from water-insoluble proteins. *Advanced Functional Materials* **2014,** *24* (38), 5962-5968.
20. Liu, F.; Tang, C.-H. Soy glycinin as food-grade Pickering stabilizers: Part. III. Fabrication of gel-like emulsions and their potential as sustained-release delivery systems for β-carotene. *Food Hydrocolloids* **2016,** *56*, 434-444.
21. Shao, Y.; Tang, C.-H. Gel-like pea protein Pickering emulsions at pH 3.0 as a potential intestine-targeted and sustained-release delivery system for β-carotene. *Food Research International* **2016,** *79*, 64-72.
22. Laguna, L.; Picouet, P.; Guàrdia, M. D.; Renard, C. M. G. C.; Sarkar, A. In vitro gastrointestinal digestion of pea protein isolate as a function of pH, food matrices, autoclaving, high-pressure and re-heat treatments. *Lwt* **2017,** *84*, 511-519.
23. George, J.; Sabapathi, S. N. Cellulose nanocrystals: synthesis, functional properties, and applications. *Nanotechnol Sci Appl* **2015,** *8*, 45-54.
24. Younas, M.; Noreen, A.; Sharif, A.; Majeed, A.; Hassan, A.; Tabasum, S.; Mohammadi, A.; Zia, K. M. A review on versatile applications of blends and composites of CNC with natural and synthetic polymers with mathematical modeling. *Int J Biol Macromol* **2019,** *124*, 591-626.
25. Li, X.; de Vries, R. Interfacial stabilization using complexes of plant proteins and polysaccharides. *Current Opinion in Food Science* **2018,** *21*, 51-56.
26. Zhou, F. Z.; Yan, L.; Yin, S. W.; Tang, C. H.; Yang, X. Q. Development of Pickering emulsions stabilized by gliadin/proanthocyanidins hybrid particles (GPHPs) and the fate of lipid oxidation and digestion. *J Agric Food Chem* **2018,** *66* (6), 1461-1471.
27. Zhang, S.; Holmes, M.; Ettelaie, R.; Sarkar, A. Pea protein microgel particles as Pickering stabilisers of oil-in-water emulsions: Responsiveness to pH and ionic strength. *Food Hydrocolloids* **2020,** *102*, 105583.
28. Minekus, M.; Alminger, M.; Alvito, P.; Ballance, S.; Bohn, T.; Bourlieu, C.; Carriere, F.; Boutrou, R.; Corredig, M.; Dupont, D.; Dufour, C.; Egger, L.; Golding, M.; Karakaya, S.; Kirkhus, B.; Le Feunteun, S.; Lesmes, U.; Macierzanka, A.; Mackie, A.; Marze, S.; McClements, D. J.; Menard, O.; Recio, I.; Santos, C. N.; Singh, R. P.; Vegarud, G. E.; Wickham, M. S.; Weitschies, W.; Brodkorb, A. A standardised static in vitro digestion method suitable for food - an international consensus. *Food Funct* **2014,** *5* (6), 1113-24.
29. Destribats, M.; Wolfs, M.; Pinaud, F.; Lapeyre, V.; Sellier, E.; Schmitt, V.; Ravaine, V. Pickering emulsions stabilized by soft microgels: influence of the emulsification process on particle interfacial organization and emulsion properties. *Langmuir* **2013,** *29* (40), 12367-74.

30. Zembyla, M.; Lazidis, A.; Murray, B. S.; Sarkar, A. Water-in-oil Pickering emulsions stabilized by synergistic particle-particle interactions. *Langmuir* **2019,** *35* (40), 13078-13089.
31. Murray, B. S. Equilibrium and dynamic surface pressure-area measurements on protein films at air-water and oil-water interfaces. *Colloids and Surfaces A: Physicochemical and Engineering Aspects* **1997,** *125* (1), 73-83.
32. Murray, B. S.; Cattin, B.; Schüler, E.; Sonmez, Z. O. Response of adsorbed protein films to rapid expansion. *Langmuir* **2002,** *18* (24), 9476-9484.
33. Murray, B. S.; Nelson, P. V. A novel Langmuir trough for equilibrium and dynamic measurements on air−water and oil−water monolayers. *Langmuir* **1996,** *12* (25), 5973-5976.
34. Anson, M. L.; Mirsky, A. E. The estimation of pepsin with hemoglobin. *J Gen Physiol* **1932,** *16* (1), 59-63.
35. Torres, O.; Murray, B. S.; Sarkar, A. Overcoming in vitro gastric destabilisation of emulsion droplets using emulsion microgel particles for targeted intestinal release of fatty acids. *Food Hydrocolloids* **2019,** *89*, 523-533.
36. Nguyen, T. T. P.; Bhandari, B.; Cichero, J.; Prakash, S. Gastrointestinal digestion of dairy and soy proteins in infant formulas: An in vitro study. *Food Research International* **2015,** *76*, 348-358.
37. Luo, Q.; Boom, R. M.; Janssen, A. E. M. Digestion of protein and protein gels in simulated gastric environment. *LWT - Food Science and Technology* **2015,** *63* (1), 161-168.
38. Opazo-Navarrete, M.; Altenburg, M. D.; Boom, R. M.; Janssen, A. E. M. The effect of gel microstructure on simulated gastric digestion of protein gels. *Food Biophys* **2018,** *13* (2), 124-138.
39. Nyemb, K.; Guérin-Dubiard, C.; Pézennec, S.; Jardin, J.; Briard-Bion, V.; Cauty, C.; Rutherfurd, S. M.; Dupont, D.; Nau, F. The structural properties of egg white gels impact the extent of in vitro protein digestion and the nature of peptides generated. *Food Hydrocolloids* **2016,** *54*, 315-327.
40. Peng, W.; Kong, X.; Chen, Y.; Zhang, C.; Yang, Y.; Hua, Y. Effects of heat treatment on the emulsifying properties of pea proteins. *Food Hydrocolloids* **2016,** *52*, 301-310.
41. Araiza-Calahorra, A.; Sarkar, A. Designing biopolymer-coated Pickering emulsions to modulate in vitro gastric digestion: a static model study. *Food Funct* **2019,** *10* (9), 5498-5509.
42. Sarkar, A.; Zhang, S.; Murray, B.; Russell, J. A.; Boxal, S. Modulating in vitro gastric digestion of emulsions using composite whey protein-cellulose nanocrystal interfaces. *Colloids Surf B Biointerfaces* **2017,** *158*, 137-146.
43. Sarkar, A.; Li, H.; Cray, D.; Boxall, S. Composite whey protein–cellulose nanocrystals at oil-water interface: Towards delaying lipid digestion. *Food Hydrocolloids* **2018,** *77*, 436-444.
44. Du Le, H.; Loveday, S. M.; Singh, H.; Sarkar, A. Pickering emulsions stabilised by hydrophobically modified cellulose nanocrystals: Responsiveness to pH and ionic strength. *Food Hydrocolloids* **2020,** *99*, 105344.
45. Ehmann, H. M.; Spirk, S.; Doliska, A.; Mohan, T.; Gossler, W.; Ribitsch, V.;

Sfiligoj-Smole, M.; Stana-Kleinschek, K. Generalized indirect fourier transformation as a valuable tool for the structural characterization of aqueous nanocrystalline cellulose suspensions by small angle X-ray scattering. *Langmuir* **2013,** *29* (11), 3740-8.
46. Scheuble, N.; Geue, T.; Windhab, E. J.; Fischer, P. Tailored interfacial rheology for gastric stable adsorption layers. *Biomacromolecules* **2014,** *15* (8), 3139-45.
47. Destribats, M.; Rouvet, M.; Gehin-Delval, C.; Schmitt, C.; Binks, B. P. Emulsions stabilised by whey protein microgel particles: towards food-grade Pickering emulsions. *Soft Matter* **2014,** *10* (36), 6941-54.
48. Andablo-Reyes, E.; Yerani, D.; Fu, M.; Liamas, E.; Connell, S.; Torres, O.; Sarkar, A. Microgels as viscosity modifiers influence lubrication performance of continuum. *Soft Matter* **2019,** *15* (47), 9614-9624.
49. Hu, H.-y.; Xing, L.-j.; Hu, Y.-y.; Qiao, C.-l.; Wu, T.; Zhou, G.-h.; Zhang, W.-g. Effects of regenerated cellulose on oil-in-water emulsions stabilized by sodium caseinate. *Food Hydrocolloids* **2016,** *52*, 38-46.
50. Wei, Y.; Cai, Z.; Wu, M.; Guo, Y.; Tao, R.; Li, R.; Wang, P.; Ma, A.; Zhang, H. Comparative studies on the stabilization of pea protein dispersions by using various polysaccharides. *Food Hydrocolloids* **2020,** *98*, 105233.
51. Bertsch, P.; Diener, M.; Adamcik, J.; Scheuble, N.; Geue, T.; Mezzenga, R.; Fischer, P. Adsorption and Interfacial Layer Structure of Unmodified Nanocrystalline Cellulose at Air/Water Interfaces. *Langmuir* **2018,** *34* (50), 15195-15202.

Supporting Information

Synergistic interactions of plant protein microgels and cellulose nanocrystals at the interface and their inhibition of gastric digestion of Pickering emulsions

*Shuning Zhang[1], Brent S. Murray[1**], Nuttaporn Suriyachay[1], Melvin Holmes[1], Rammile Ettelaie[1], Anwesha Sarkar[1*]*

[1] Food Colloids and Bioprocessing Group, School of Food Science and Nutrition, University of Leeds, Woodhouse Lane, Leeds LS2 9JT, UK

*Corresponding author:

Prof. Anwesha Sarkar (Email: A.Sarkar@leeds.ac.uk)

**Joint Corresponding author: Prof. Brent S. Murray (Email: B.S.Murray@leeds.ac.uk)

Food Colloids and Bioprocessing Group,

School of Food Science and Nutrition, University of Leeds, Woodhouse Lane, Leeds LS2 9JT, UK.

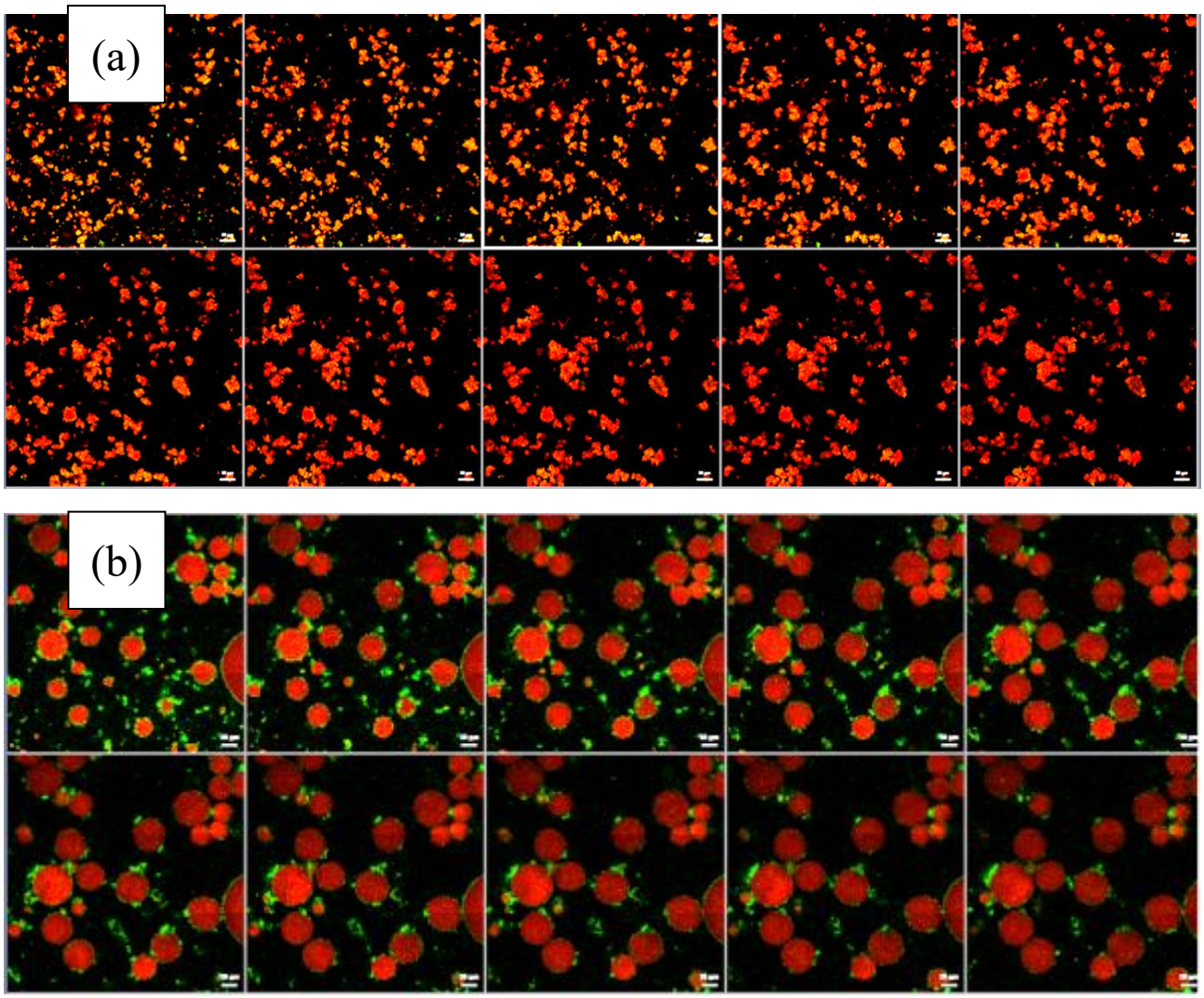

Figure S1. Confocal micrograph tiles covering different fields within the sample of 20 wt% oil-in-water emulsions stabilized by PPM (PPM-E) after (a) 0 min and (b) 120 min of *in vitro* gastric digestion at pH 3.0. Green colour represents PPM (stained by Nile Blue); red colour represents the oil phase (stained by Nile Red); black colour represents air or water. Note 0 min in Figure (a) represents the PPM-E+SGF mixture at pH 3.0 *without* the addition of pepsin. Scale bar represents 20 μm.

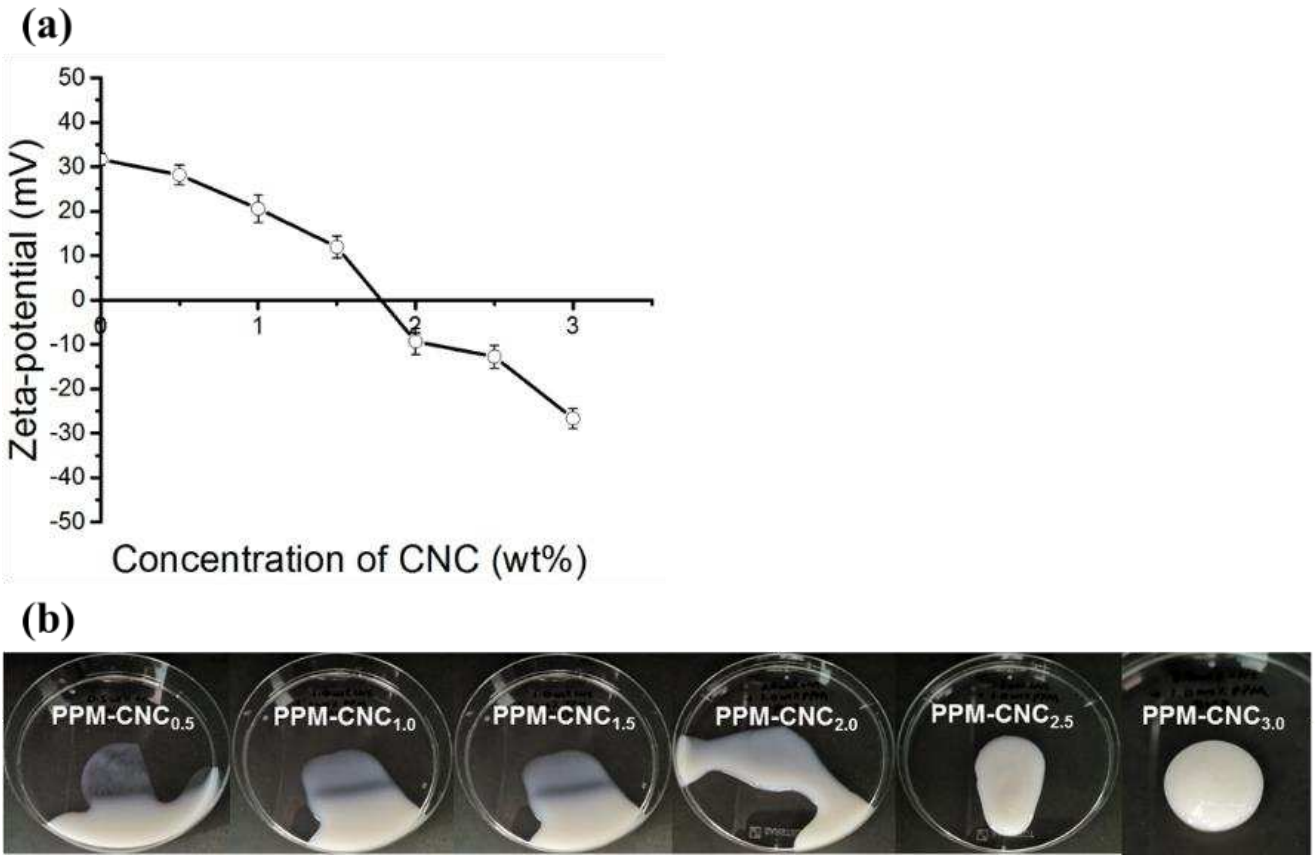

Figure S2. Influence of concentration of cellulose nanocrystals (CNC) on: (a) the mean ζ-potential values (○) of aqueous dispersion of PPM and (b) the flowability of these mixtures. Error bars represent standard deviations.

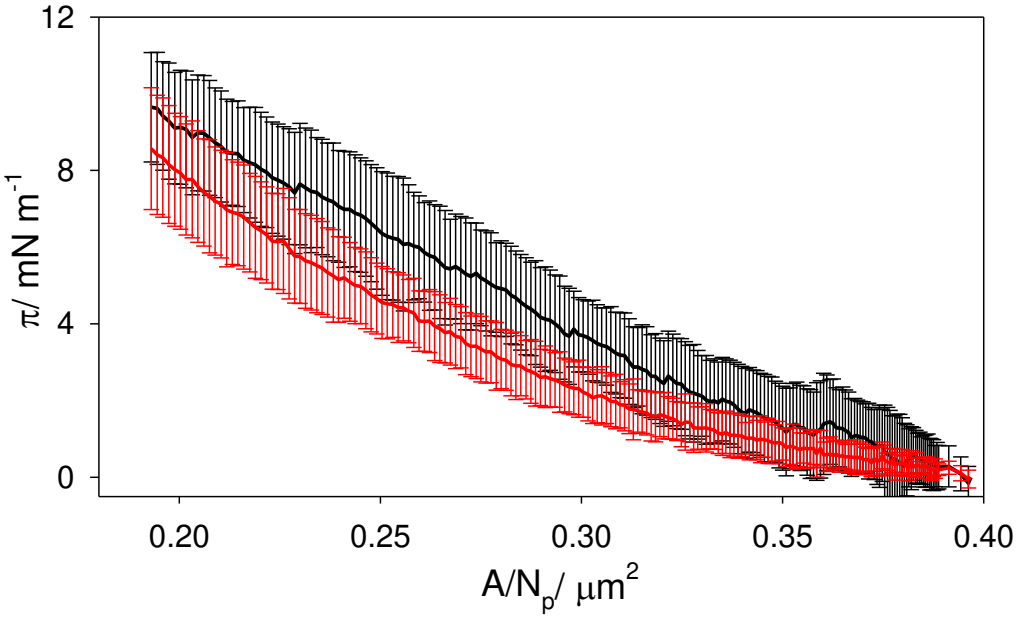

Figure S3. Surface pressure (π) versus area per particle (A/N_p) spread at the A-W interface for 0.466 wt% PPM: standard deviations about the means are shown for 9 separate compressions at pH 7.0 (black line and error bars) and pH 3.0 (red line and error bars).

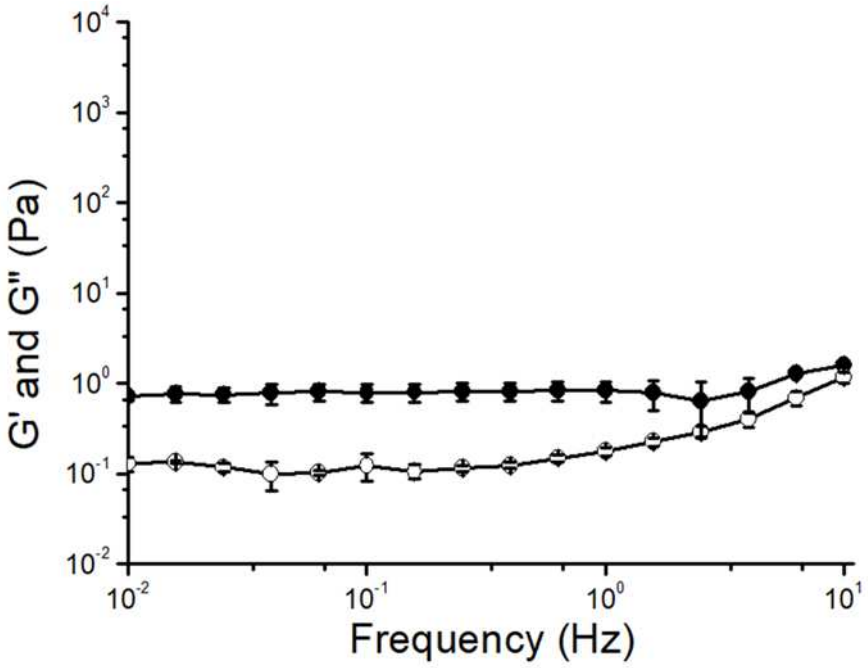

Figure S4. Frequency sweep curves of freshly prepared 20 wt% O/W emulsions stabilized by PPM (PPM-E) at pH 3.0 (G′●, G′′○). Error bars represent standard deviations.

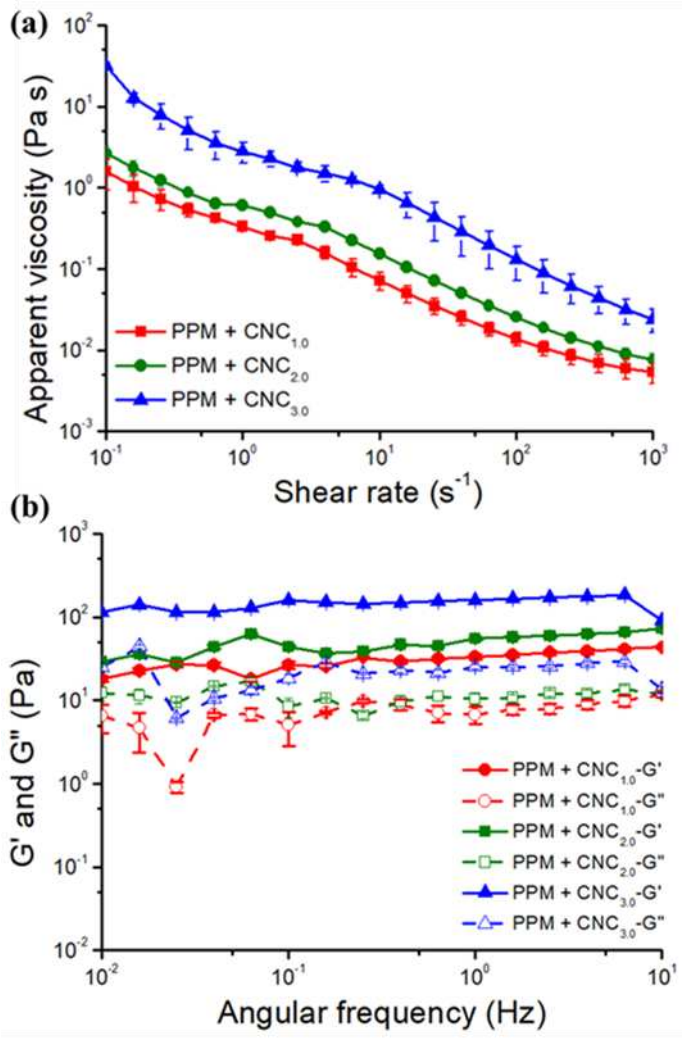

Figure S5. (a) Flow curves and (b) frequency sweep curves of freshly prepared PPM (1 wt%) at pH 3 mixed with 1 wt% CNC (PPM + $CNC_{1.0}$) (●), 2 wt% CNC (PPM + $CNC_{2.0}$) (■) and 3 wt% CNC (PPM + $CNC_{3.0}$) (▲). These samples are aqueous dispersions of particles without any oil droplets. Error bars represent standard deviations.

Table S1. Mean droplet size of PPM-E with 1, 2 and 3 wt% CNC after 0, 30 and 120 min *in vitro* gastric digestion. Time 0 min represents the emulsion + SGF mixture at pH 3.0 without the addition of pepsin. Different superscripts (a-b) in the same column indicate significant differences between different samples at $p < 0.05$ level.

Size (μm)		**Digestion time (min)**		
		0	**30**	**120**
PPM-E + $CNC_{1.0}$	d_{32}	4.0 ± 0.1^{a}	3.3 ± 0.2^{b}	3.2 ± 0.3^{b}
	d_{43}	18.0 ± 4.7^{a}	14.6 ± 3.7^{a}	12.3 ± 1.8^{a}
PPM-E + $CNC_{2.0}$	d_{32}	3.2 ± 0.2^{a}	3.1 ± 0.2^{a}	2.7 ± 0.2^{b}
	d_{43}	13.9 ± 1.9^{a}	13.1 ± 1.9^{a}	9.4 ± 1.7^{b}
PPM-E + $CNC_{3.0}$	d_{32}	3.2 ± 0.4^{a}	3.1 ± 0.3^{a}	2.4 ± 0.1^{b}
	d_{43}	17.6 ± 4.9^{a}	16.4 ± 4.9^{a}	8.1 ± 1.4^{b}